

# Functional and Physical Interaction of Diacylglycerol Kinase $\zeta$ with Protein Kinase $C\alpha$ Is Required for Cerebellar Long-Term Depression

Dongwon Lee,<sup>1,2</sup> Yukio Yamamoto,<sup>2</sup> Eunjoon Kim,<sup>1,3</sup> and Keiko Tanaka-Yamamoto<sup>2</sup>

<sup>1</sup>Department of Biological Sciences, Korea Advanced Institute of Science and Technology, Daejeon 305-701, Korea, <sup>2</sup>Center for Functional Connectomics, Korea Institute of Science and Technology, Seoul 136-791, Korea, and <sup>3</sup>Center for Synaptic Brain Dysfunctions, Institute for Basic Science, Daejeon 305-701, Korea

The balance between positive and negative regulators required for synaptic plasticity must be well organized at synapses. Protein kinase  $C\alpha$  (PKC $\alpha$ ) is a major mediator that triggers long-term depression (LTD) at synapses between parallel fibers and Purkinje cells in the cerebellum. However, the precise mechanisms involved in PKC $\alpha$  regulation are not clearly understood. Here, we analyzed the role of diacylglycerol kinase  $\zeta$  (DGK $\zeta$ ), a kinase that physically interacts with PKC $\alpha$  as well as postsynaptic density protein 95 (PSD-95) family proteins and functionally suppresses PKC $\alpha$  by metabolizing diacylglycerol (DAG), in the regulation of cerebellar LTD. In Purkinje cells of DGK $\zeta$ -deficient mice, LTD was impaired and PKC $\alpha$  was less localized in dendrites and synapses. This impaired LTD was rescued by virus-driven expression of wild-type DGK $\zeta$ , but not by a kinase-dead mutant DGK $\zeta$  or a mutant lacking the ability to localize at synapses, indicating that both the kinase activity and synaptic anchoring functions of DGK $\zeta$  are necessary for LTD. In addition, experiments using another DGK $\zeta$  mutant and immunoprecipitation analysis revealed an inverse regulatory mechanism, in which PKC $\alpha$  phosphorylates, inactivates, and then is released from DGK $\zeta$ , is required for LTD. These results indicate that DGK $\zeta$  is localized to synapses, through its interaction with PSD-95 family proteins, to promote synaptic localization of PKC $\alpha$ , but maintains PKC $\alpha$  in a minimally activated state by suppressing local DAG until its activation and release from DGK $\zeta$  during LTD. Such local and reciprocal regulation of positive and negative regulators may contribute to the fine-tuning of synaptic signaling.

**Key words:** cerebellum; DGK $\zeta$ ; long-term depression; PKC $\alpha$ ; Purkinje cells

## Significance Statement

Many studies have identified signaling molecules that mediate long-term synaptic plasticity. In the basal state, the activities and concentrations of these signaling molecules must be maintained at low levels, yet be ready to be boosted, so that synapses can undergo synaptic plasticity only when they are stimulated. However, the mechanisms involved in creating such conditions are not well understood. Here, we show that diacylglycerol kinase  $\zeta$  (DGK $\zeta$ ) creates optimal conditions for the induction of cerebellar long-term depression (LTD). DGK $\zeta$  works by regulating localization and activity of protein kinase  $C\alpha$  (PKC $\alpha$ ), an important mediator of LTD, so that PKC $\alpha$  effectively responds to the stimulation that triggers LTD.

## Introduction

Many forms of long-term synaptic plasticity have been observed in several brain areas, which are triggered by increases in concen-

trations or activities of signaling molecules that work positively for synaptic plasticity (Huganir and Nicoll, 2013). In contrast, molecules that negatively regulate these positive regulators are also implicated in synaptic plasticity (Baumgärtel and Mansuy, 2012). One way such negative regulators are thought to be in-

Received May 20, 2015; revised Sept. 28, 2015; accepted Oct. 18, 2015.

Author contributions: E.K. and K.T.-Y. designed research; D.L. and Y.Y. performed research; D.L. analyzed data; D.L. and K.T.-Y. wrote the paper.

This work was supported by the World Class Institute (WCI) Program of the National Research Foundation of Korea (NRF) funded by the Ministry of Education, Science and Technology of Korea (NRF Grant WCI 2009-003), Japan Science and Technology Agency PRESTO Grant, Korea Institute of Science and Technology Institutional Program Project 2E25540, the Takeda Science Foundation, the Research Foundation for Opto-Science and Technology, NRF of Korea Global Ph.D. Fellowship Program funded by the Ministry of Education, Science and Technology of Korea NRF Grant 20110007460, and Institute for Basic Science IBS-R002-D1. We thank Dr. George J. Augustine for valuable

comments on this paper; Yoonhee Kim and Begüm Aküzüm for technical assistance; and Dr. Karam Kim for helpful suggestions on experiments using DGK $\zeta$ <sup>-/-</sup> mice.

The authors declare no competing financial interests.

Correspondence should be addressed to Dr. Keiko Tanaka-Yamamoto, Center for Functional Connectomics, Korea Institute of Science and Technology, 39-1 Hawolgok-dong, Seongbuk-gu, Seoul 136-791, Korea. E-mail: keikoyamat@gmail.com.

DOI:10.1523/JNEUROSCI.1991-15.2015

Copyright © 2015 the authors 0270-6474/15/3515453-13\$15.00/0

involved is by maintaining low activities of positive regulators at a basal state; yet the inhibitory effects of these negative regulators are reduced upon the induction of synaptic plasticity (Fukunaga et al., 2000; Launey et al., 2004). Another function of negative regulators is to prevent the hyperactivation of positive regulators, which oppositely reduces the probability to induce synaptic plasticity (Khoutorsky et al., 2013). The balance between positive and negative regulators appears to be important to achieve appropriate activities of the signaling network that triggers synaptic plasticity.

In the case of long-term depression (LTD) at synapses between parallel fibers (PFs) and Purkinje cells in the cerebellum, a large number of signaling molecules have been implicated to be involved (Ito, 2002; Hirano, 2013; Kim and Tanaka-Yamamoto, 2013). Many of these molecules can be categorized as positive regulators, and protein kinase C (PKC) has long been known to be necessary and even sufficient for LTD (Linden and Connor, 1991; Hartell, 1994; De Zeeuw et al., 1998; Endo and Launey, 2003; Kondo et al., 2005). Although the pathway and functions of PKC activation during LTD have been well understood (Hirano, 2013; Kim and Tanaka-Yamamoto, 2013), it is not clear as to how PKC activity is precisely regulated. Another question remains regarding isoform specificity. Although at least 8 isoforms of PKC are expressed in Purkinje cells, PKC $\alpha$  has been reported to be responsible for LTD. The unique PDZ ligand motif in the C terminus of PKC $\alpha$  was shown to be important for its function in LTD (Leitges et al., 2004), suggesting that its binding with the PDZ-domain containing protein PICK1 via this PDZ ligand motif (Staudinger et al., 1997) may be required for its involvement in LTD. However, because PICK1 appears to bind only with activated PKC $\alpha$  (Perez et al., 2001), comprehensive mechanisms explaining the specificity of PKC $\alpha$  remain unclear.

Diacylglycerol kinase (DGK) metabolizes diacylglycerol (DAG) to phosphatidic acid (PA), which is the major pathway to terminate DAG signaling (Sakane et al., 2007; Cai et al., 2009). Therefore, DGK can be considered a negative regulator of PKC, which can be activated by DAG. The DGK isoform DGK $\zeta$  was shown to be targeted to excitatory synapses by its interaction with postsynaptic density protein-95 (PSD-95) family proteins and to regulate synaptic morphology and functions in hippocampal pyramidal neurons (K. Kim et al., 2009, 2010; Seo et al., 2012). In a study using an *in vitro* assay and cultured cell lines, it was demonstrated that DGK $\zeta$  reduces PKC $\alpha$  activity by interacting with PKC $\alpha$  and metabolizing DAG, whereas such regulation of PKC $\alpha$  by DGK $\zeta$  is attenuated by PKC $\alpha$ -dependent phosphorylation of DGK $\zeta$  and by subsequent dissociation of PKC $\alpha$  from DGK $\zeta$  (Luo et al., 2003a,b). Given that DGK $\zeta$  is expressed at high levels in cerebellar Purkinje cells (Hozumi et al., 2003; K. Kim et al., 2009), the mutual regulation of DGK $\zeta$  and PKC $\alpha$  may be crucial for the local and fine regulation of PKC $\alpha$  activity at synapses upon the stimulation triggering LTD.

In this study, we investigated the involvement of DGK $\zeta$  in cerebellar LTD using DGK $\zeta$ -deficient (DGK $\zeta^{-/-}$ ) mice. We found that DGK $\zeta$  contributes to LTD by regulating the synaptic localization and activities of PKC $\alpha$ , and by releasing PKC $\alpha$  during LTD. Our study demonstrates a novel signaling mechanism that effectively responds to synaptic stimulation via physical and functional interactions between DGK $\zeta$  and PKC $\alpha$ .

## Materials and Methods

**Mice.** All procedures involving mice were performed according to the guidelines of the Institutional Animal Care and Use Committee of Korea Institute of Science and Technology. In this study, we used DGK $\zeta^{-/-}$

mice, which were generated previously (Zhong et al., 2003). For experiments comparing electrophysiological and biochemical properties between wild-type (DGK $\zeta^{+/+}$ ) and DGK $\zeta^{-/-}$  mice, heterozygous (DGK $\zeta^{+/-}$ ) mice were crossed to produce both DGK $\zeta^{+/+}$  and DGK $\zeta^{-/-}$  littermates. Lentiviral or adeno-associated viral (AAV) vectors were stereotaxically injected into the cerebellar cortex of 9- to 11-day-old DGK $\zeta^{-/-}$  pups. The injected pups were taken care of by foster ICR female mice with pups of similar age.

**Patch-clamp recording and live cell imaging.** Chemicals used were obtained from Sigma or Wako Pure Chemical Industries, unless otherwise specified. Whole-cell patch-clamp recordings were made from Purkinje cells as described previously (Miyata et al., 2000; Wang et al., 2000). Briefly, sagittal slices (200  $\mu$ m) of cerebella from 17- to 25-day-old mice of either sex were bathed in extracellular solution (ACSF) containing the following (in mM): 125 NaCl, 2.5 KCl, 1.3 MgCl<sub>2</sub>, 2 CaCl<sub>2</sub>, 1.25 NaH<sub>2</sub>PO<sub>4</sub>, 26 NaHCO<sub>3</sub>, 20 glucose, and 0.01 bicuculline methochloride (Tocris Bioscience). Patch pipettes (resistance 5–6 M $\Omega$ ) were filled with the following (in mM): 130 potassium gluconate, 2 NaCl, 4 MgCl<sub>2</sub>, 4 Na<sub>2</sub>-ATP, 0.4 Na-GTP, 20 HEPES, pH 7.2, and 0.25 EGTA. To visualize increases in intracellular calcium concentrations ([Ca<sup>2+</sup>]<sub>i</sub>), Oregon Green 488 BAPTA-1 (OGB1, Invitrogen, 0.25 mM) was added instead of EGTA. When GFP-conjugated proteins were virally expressed, whole-cell patch-clamp recordings were made from Purkinje cells expressing GFP, which were identified by GFP fluorescence under a microscope (Olympus BX61WI). The imaging of GFP was performed using a confocal microscope (Olympus FV1000).

EPSCs were evoked in Purkinje cells (holding potential of  $-70$  mV) by activating PFs with a glass stimulating electrode on the surface of the molecular layer (PF-EPSCs). PF-EPSCs were acquired and analyzed using pClamp software (Molecular Devices). To evoke LTD by electrical stimulation (PF $\Delta$ V), PF stimuli were paired with Purkinje cell depolarization (0 mV, 200 ms), 300 $\times$  at 1 Hz. To test the effects of a shorter (200 PF $\Delta$ V) or longer (500 PF $\Delta$ V) duration of stimulation, the same stimulus was applied 200 or 500 times at 1 Hz, respectively. For the induction of long-term potentiation (LTP, PF), only PF stimuli were applied 300 $\times$  at 1 Hz. Data were accepted if the series resistance changed by <20%, the input resistance was >80 M $\Omega$ , and the holding current changed by <20%. Miniature EPSCs (mEPSCs) were recorded as described previously (Yamamoto et al., 2012). To detect slow EPSCs, a burst of PF stimulation (100 Hz, 100 ms) was applied in the presence of the AMPAR antagonist CNQX (25  $\mu$ M, Tocris Bioscience) (Hartmann et al., 2008).

Live cell imaging of OGB1 was performed using a microscope (Nikon Eclipse FN1) equipped with an iXon Ultra 897 camera (Andor) and NIS elements imaging software (Nikon). Images of the cells were taken at 30 Hz, before, during, and after the PF burst stimulation (100 Hz, 100 ms). The timing of PF stimulation was controlled by the trigger-out feature of NIS elements software. The ratio of increased fluorescence to basal fluorescence ( $\Delta F/F_0$ ) was calculated from the stimulated Purkinje cell dendrites using the equation  $\Delta F/F_0 = ((F - F_b) - (F_0 - F_b))/(F_0 - F_b)$ , in which F, F<sub>0</sub>, and F<sub>b</sub> are fluorescence intensity in the ROI at a certain time point, averaged intensity in the ROI before the PF stimulation, and background signals, respectively.

**Immunoprecipitation, immunoblotting, immunohistochemistry, and biocytin labeling.** Primary antibodies used were rabbit or guinea pig anti-DGK $\zeta$  (K. Kim et al., 2009), mouse anti-PKC $\alpha$  (BD Biosciences), mouse (Sigma), rabbit (Sigma), or guinea pig (Synaptic Systems) anti-calbindin, mouse anti-metabotropic glutamate receptor 1 (mGluR1, BD Biosciences), mouse anti-FLAG (M2, Sigma), rabbit anti-synapsin 1/2 (Synaptic Systems), mouse anti- $\beta$ -actin (Santa Cruz Biotechnology), rabbit anti-mitogen-activated protein kinase/extracellular signal-regulated kinases (MAPK/Erk, Cell Signaling Technology), rabbit anti-phosphorylated MAPK (Cell Signaling Technology), rabbit anti-GluA2 (Millipore), rabbit anti-PICK1 (Abcam), and rabbit anti-PSD-93/chapsyn-110 (1634) (M.H. Kim et al., 2009) antibodies. Secondary antibodies used were HRP-conjugated anti-mouse or anti-rabbit IgG (GE Healthcare), HRP-conjugated anti-guinea pig IgG (Jackson ImmunoResearch Laboratories), AlexaFluor-647-conjugated anti-mouse IgG (Jackson ImmunoResearch Laboratories), AlexaFluor-647-conjugated anti-rabbit IgG (Invitrogen), AlexaFluor-488-conjugated anti-rabbit,

anti-mouse, or anti-guinea pig IgG (Invitrogen), and AlexaFluor-405-conjugated anti-rabbit IgG (Invitrogen) antibodies.

Immunoprecipitation analyses using cerebellar slices were performed as described previously with slight modifications (Yamamoto et al., 2012). Briefly, freshly prepared cerebellar slices were subjected to chemical LTD stimulation after incubating for 30 min in normal ACSF. For chemical LTD stimulation, slices were treated with extracellular solution containing 50 mM K<sup>+</sup> and 10  $\mu$ M glutamate (K-glu) for 5 min. Slices were then lysed in lysis buffer containing the following: 150 mM NaCl, 50 mM Tris, pH 8, 1 mM EDTA, 1% Triton X-100, 10% glycerol, 1  $\mu$ M staurosporine (Calbiochem), 1  $\times$  proteinase inhibitor mixture (Nacalai Tesque), and 1  $\times$  phosphatase inhibitor mixture (Nacalai Tesque). After homogenization and centrifugation, mouse anti-PKC $\alpha$  was added to the supernatant (~500  $\mu$ g protein) to immunoprecipitate PKC $\alpha$  and rotated at 4°C followed by the addition of 20  $\mu$ l protein G-Sepharose (GE Healthcare). The immunoprecipitate was suspended in SDS-PAGE sample buffer and subjected to immunoblotting analyses to detect DGK $\zeta$  and PKC $\alpha$ . To quantify the binding of PKC $\alpha$  to DGK $\zeta$ , band intensities were measured using ImageJ software (National Institutes of Health, <http://imagej.nih.gov/ij/>), and the ratios of normalized band intensities of DGK $\zeta$  to those of PKC $\alpha$  were then calculated. The binding between DGK $\zeta$  and PSD-93 in the cerebellum was confirmed by immunoprecipitation with a PSD-93 antibody of cerebellar lysates that were solubilized by 1% sodium deoxycholate (K. Kim et al., 2009).

To test the binding between DGK $\zeta$  and PKC $\alpha$ , human embryonic kidney (HEK) 293T cells were transfected with pcDNA3-FLAG-DGK $\zeta$  (wild-type) and pcDNA3-PKC $\alpha$  (wild-type or mutant). Approximately 45 h after transfection, cells were lysed in lysis buffer containing the following: 150 mM NaCl, 50 mM Tris, pH 8, 1 mM EDTA, 0.2% NP-40 Alternative (Calbiochem), 10% glycerol, 1  $\times$  proteinase inhibitor mixture, and 1  $\times$  phosphatase inhibitor mixture. Cell lysates were centrifuged to remove cell debris, and the supernatant was used for immunoprecipitation using M2 FLAG beads (Sigma). The immunoprecipitates were then subjected to immunoblotting analyses to detect FLAG-tagged DGK $\zeta$  and PKC $\alpha$ .

Crude synaptosome (P2) and cytosolic fractions (S2) were prepared as described previously (Kohda et al., 2013). In brief, the whole cerebellum from DGK $\zeta$ <sup>+/+</sup> or DGK $\zeta$ <sup>-/-</sup> mice was dissected out and homogenized in HEPES-buffered sucrose (0.32 M sucrose, 5 mM HEPES, pH 7.3, 0.1 mM EDTA, 1  $\times$  proteinase inhibitor mixture, and 1  $\times$  phosphatase inhibitor mixture). After removal of the nuclear fraction by centrifugation at 1000  $\times$  g for 5 min, the supernatant was centrifuged at 12,000  $\times$  g for 20 min. The resulting pellet was suspended in HEPES-buffered sucrose, and the supernatant and the suspended pellet were used as S2 and P2 fractions, respectively. The S2 and P2 fractions were mixed with SDS-PAGE sample buffer and subjected to immunoblotting analyses to detect PKC $\alpha$ ,  $\beta$ -actin, synapsin, AMPAR subunit GluA2, DGK $\zeta$ , and PICK1. For quantification, band intensities were measured using ImageJ software. Because the ratios of the band intensities of  $\beta$ -actin in the P2 fractions to those in the S2 fractions did not significantly differ between DGK $\zeta$ <sup>+/+</sup> and DGK $\zeta$ <sup>-/-</sup> cerebella ( $p = 0.197$ , Student's  $t$  test), the band intensities of PKC $\alpha$ , synapsin, and GluA2 were normalized to those of  $\beta$ -actin. Then, the ratios of the normalized band intensities in the P2 fractions to those in the S2 fractions were calculated ( $r = (X_{P2}/\beta - \text{actin}_{P2}) / (X_{S2}/\beta - \text{actin}_{S2})$ , where  $X_{P2}$  and  $X_{S2}$  are the band intensities of PKC $\alpha$ , synapsin, or GluA2 in the P2 and S2 fractions, respectively, and  $\beta$ -actin<sub>P2</sub> and  $\beta$ -actin<sub>S2</sub> are the band intensities of  $\beta$ -actin in the P2 and S2 fractions, respectively).

For the labeling of Purkinje cells using biocytin, whole-cell patch clamps were made with internal solution including 0.5% biocytin (Tocris Bioscience) and AlexaFluor-488 (Invitrogen). After waiting 20 min for the diffusion of the internal solution into Purkinje cells, slices were immediately fixed with 4% PFA, permeabilized with 0.1% Triton X-100, and incubated with AlexaFluor-488-conjugated streptavidin (1:500, Invitrogen). Z-stack images of single Purkinje cells and digitally magnified images of distal dendrites were acquired by an A1R laser-scanning confocal microscope (Nikon) for Sholl analysis and the counting of spine numbers, respectively.

For immunohistochemistry of cerebellar slices, mice were anesthetized and perfused transcardially with 4% PFA in 0.1 M sodium phosphate buffer, pH 7.4. The cerebellum was postfixed for 3 h at 4°C, followed by sectioning (40  $\mu$ m) using a vibrating microtome (Leica VT 1200S). Sections were blocked in 5% normal goat serum in PBS, incubated in primary antibodies overnight at 4°C, washed several times, and then incubated in secondary antibodies for 3 h at room temperature. Single optical sections of confocal images were acquired by an A1R laser scanning confocal microscope.

To analyze MAPK phosphorylation, freshly prepared cerebellar slices were subjected to chemical LTD stimulation for 5 min and washed in normal ACSF for 0–10 min. Slices were then lysed in the same lysis buffer as that used for immunoprecipitation analyses. After homogenization, samples were centrifuged to remove cell debris. The lysate was subjected to SDS-PAGE to detect MAPK and phosphorylated MAPK by immunoblotting. To quantify MAPK phosphorylation, band intensities were measured by ImageJ, and the ratio of phosphorylated MAPK to total MAPK was then calculated.

*In vivo viral injection.* To make lentiviral vectors, constructs for vesicular stomatitis virus G-pseudotyped lentiviral vectors were provided by St. Jude Children's Research Hospital (Hanawa et al., 2002). Viral vectors that express GFP-DGK $\zeta$ -WT or GFP-DGK $\zeta$ - $\Delta$ C under the control of the murine stem cell virus (MSCV) promoter were produced as described previously (Torashima et al., 2006) with slight modifications. In brief, HEK293T cells were cotransfected with a mixture of four plasmids, pCAGkGP1R, pCAG4RTR2, pCAG-vesicular stomatitis virus G, and either pCL20c-MSCV-GFP-DGK $\zeta$ -WT or pCL20c-MSCV-GFP-DGK $\zeta$ - $\Delta$ C, using calcium phosphate. At ~46 h after transfection, viral vectors were harvested from the culture medium by ultracentrifugation at 25,000 rpm for 90 min, suspended in Hanks balanced salt solution, and stored at -80°C.

To make AAV vectors, an AAV vector plasmid with the Ca<sup>2+</sup>/calmodulin-dependent protein kinase II  $\alpha$  (CaMKII $\alpha$ ) promoter that was developed by the Deisseroth laboratory was obtained from Addgene. AAV vectors were produced according to the protocol provided by the Salk Institute Gene Transfer, Targeting and Therapeutics core facility (<http://vectorcore.salk.edu/index.php>) with slight modifications. In brief, HEK293T cells were cotransfected with a mixture of three plasmids: pHelper (Agilent Technologies), serotype 1 plasmid (a gift from Dr. Jinyun Kim, Korea Institute of Science and Technology), and pAAV-CaMKII $\alpha$ -GFP, pAAV-CaMKII $\alpha$ -GFP-DGK $\zeta$ -WT, pAAV-CaMKII $\alpha$ -GFP-DGK $\zeta$ -KD, or pAAV-CaMKII $\alpha$ -GFP-DGK $\zeta$ -SN using calcium phosphate. At ~72 h after transfection, cells were harvested and lysed by sonication. Then, AAV vectors were collected from the cell lysate by gradient ultracentrifugation using a Beckman NVT90 rotor at 48,000 rpm for 47 min, dialyzed in PBS with sucrose, concentrated by centrifugal filter devices (Millipore), and stored at -80°C.

Viral vectors were injected into the cerebellum of 9- to 11-day-old DGK $\zeta$ <sup>-/-</sup> pups, as described previously (Torashima et al., 2006) with slight modifications. Briefly, mice were anesthetized by Avertin (250  $\mu$ g/g body weight) and mounted on a stereotaxic stage. The cranium over the cerebellar vermis was exposed by a midline sagittal incision. A hole was made ~3 mm caudal from  $\lambda$  by the tip of forceps, and a glass needle was placed in lobe IV-V of the cerebellar vermis. The lentiviral solution (2–3  $\mu$ l total) was injected at a rate of 200 nl/min, and the AAV solution (1  $\mu$ l total) was injected at three different locations at a rate of 1000 nl/min, using an UltraMicroPump II and Micro4 controller (World Precision Instruments). After the surgery, mice were kept on a heating pad until they recovered from the anesthesia, and then they were returned to their foster ICR mother.

*Statistical analysis.* Statistical differences were determined by the paired or unpaired Student's  $t$  test (for two-group comparisons) and one-way or two-way ANOVA followed by the Tukey or Bonferroni test (for more than two-group comparisons). Statistical analysis of mEPSC amplitude was performed by the Mann-Whitney test. Analyses were performed using GraphPad Prism 6 software.

## Results

### DGK $\zeta$ expression in cerebellar

#### Purkinje cells

We first confirmed the expression of DGK $\zeta$  in the cerebellum by Western blot analysis of cerebellar lysates of DGK $\zeta^{+/+}$  mice (Fig. 1A). To investigate the distribution of endogenous DGK $\zeta$  in the cerebellum, we performed immunohistochemical staining of sagittal cerebellar slices. Consistent with previous reports (Hozumi et al., 2003; K. Kim et al., 2009), the immunosignal of DGK $\zeta$  was predominantly detected in cerebellar Purkinje cells in DGK $\zeta^{+/+}$  mice (Fig. 1B,C). Magnified images around distal dendrites showed that DGK $\zeta$  also exists in the distal dendrites of Purkinje cells as well as their protrusive structures (Fig. 1D,E). We confirmed that these protrusions are dendritic spines by their overlap with mGluR1 (Fig. 1F), which is concentrated on dendritic spines (Takács et al., 1997; Yoshida et al., 2006). In contrast, we did not detect clear signals in DGK $\zeta^{-/-}$  mice by both Western blot (Fig. 1A) and immunohistochemical (Fig. 1G) analyses, confirming that the DGK $\zeta$  antibody used in this study (K. Kim et al., 2009) specifically detects DGK $\zeta$ . These data indicate that DGK $\zeta$  is strongly expressed in cerebellar Purkinje cells. Because DGK $\zeta$  exists not only in soma and proximal dendrites, but also in distal dendrites and dendritic spines of Purkinje cells, DGK $\zeta$  might play roles in the regulation of Purkinje cell synapses.

#### Cerebellar LTD is impaired in DGK $\zeta^{-/-}$ mice

To investigate whether DGK $\zeta$  plays a role in the regulation of cerebellar Purkinje cell synapses, we compared basal synaptic transmission at PF-Purkinje cell synapses between DGK $\zeta^{+/+}$  and DGK $\zeta^{-/-}$  mice (Fig. 2A). The kinetics of EPSC were not different between DGK $\zeta^{+/+}$  and DGK $\zeta^{-/-}$  mice (10%–90% rise time: DGK $\zeta^{+/+}$ ,  $2.37 \pm 0.2$  ms,  $n = 10$ ; DGK $\zeta^{-/-}$ ,  $2.03 \pm 0.11$  ms,  $n = 9$ ,  $p = 0.171$ ; decay time constant: DGK $\zeta^{+/+}$ ,  $11.9 \pm 1.1$  ms,  $n = 10$ ; DGK $\zeta^{-/-}$ ,  $10.4 \pm 0.7$  ms,  $n = 9$ ,  $p = 0.24$ , Student's  $t$  test). The relationship between the stimulus intensity and the amplitude of PF-EPSC was also unchanged in DGK $\zeta^{-/-}$  mice (Fig. 2B,  $p = 0.926$ , two-way ANOVA). Consistently, distributions of mEPSC amplitudes recorded in DGK $\zeta^{-/-}$  mice were equivalent to those in DGK $\zeta^{+/+}$  mice, and their averaged amplitudes were not significantly different (Fig. 2C,  $p = 0.061$ , Mann-Whitney test), indicating that the amplitude of PF-EPSC was not affected by the lack of DGK $\zeta$ . Likewise, presynaptic glutamate release did not appear to be affected because the paired-pulse facilitation (PPF) ratio of PF-EPSC in DGK $\zeta^{-/-}$  mice was comparable with that in DGK $\zeta^{+/+}$  mice (Fig. 2D,  $p = 0.745$ , two-way ANOVA). In addition,

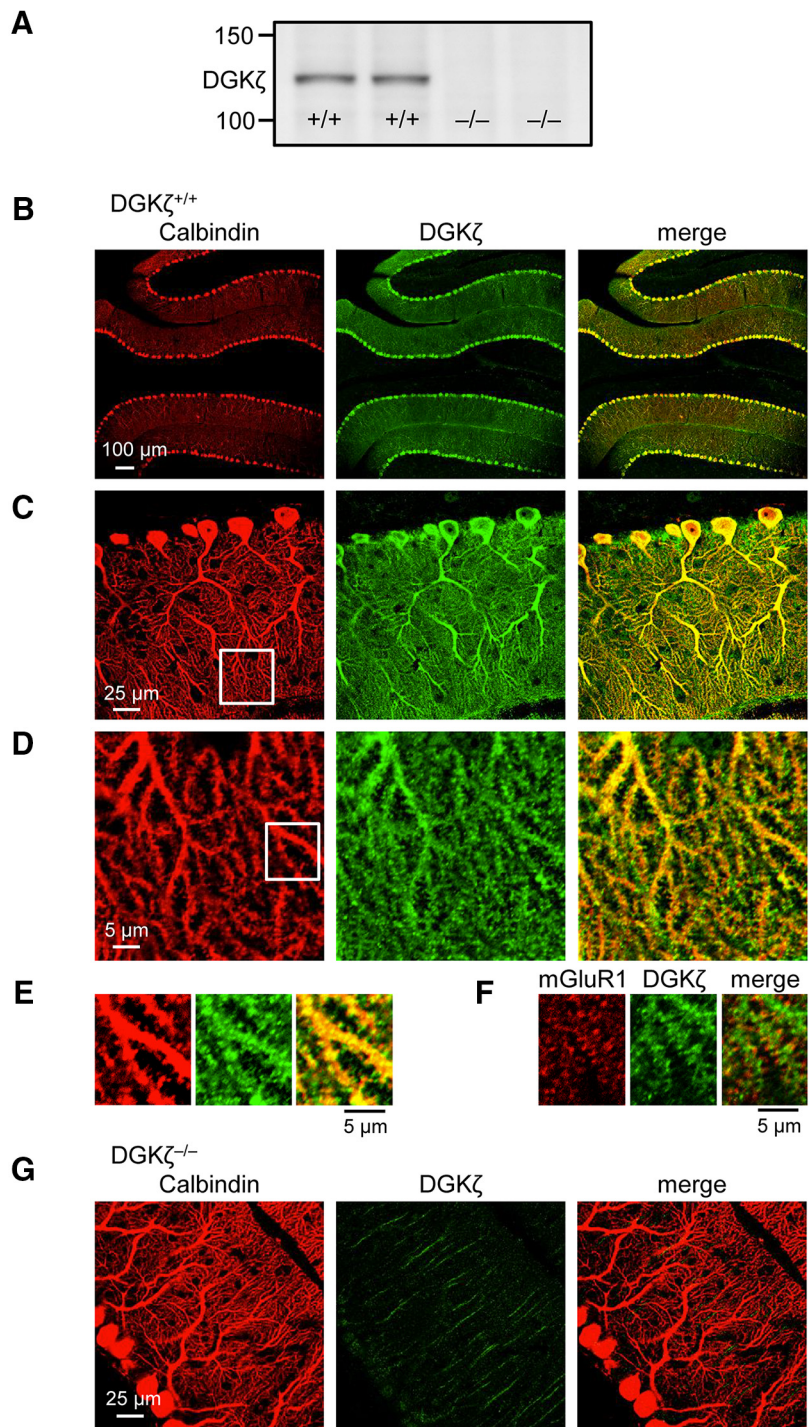


**Figure 1.** Expression of DGK $\zeta$  in cerebellar Purkinje cells. **A**, Immunoblot using an antibody against DGK $\zeta$  in cerebellar lysates of two DGK $\zeta^{+/+}$  and two DGK $\zeta^{-/-}$  mice. **B–G**, Confocal images of DGK $\zeta^{+/+}$  (**B–F**) or DGK $\zeta^{-/-}$  (**G**) cerebellar slices double stained with antibodies against calbindin (red) and DGK $\zeta$  (green; **B–E**, **G**) or with antibodies against mGluR1 (red) and DGK $\zeta$  (green; **F**).

we investigated the spine density by visualizing dendritic spines of Purkinje cells using biocytin, which was introduced through a patch pipette. We found that there was no significant difference in spine density between DGK $\zeta^{+/+}$  and DGK $\zeta^{-/-}$  mice (Fig. 2E,  $p = 0.7$ , Student's  $t$  test). Thus, DGK $\zeta$  deficiency does not affect basal synaptic transmission and synaptic density at PF-Purkinje cell synapses. This is in clear contrast to the case of hippocampal synapses, in which spine density and excitatory synaptic transmission are re-

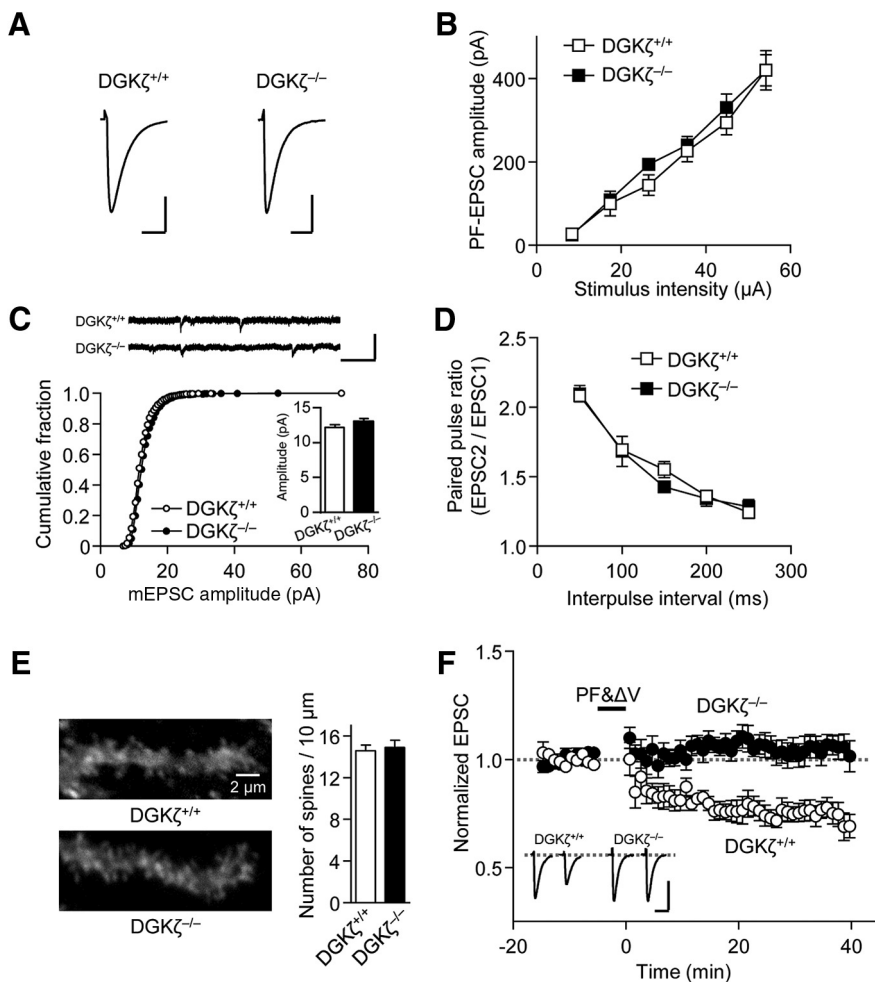


**Figure 2.** DGK $\zeta$  deficiency impairs cerebellar LTD but has no effect on basal transmission, presynaptic release, and spine density. **A**, Averaged traces of PF-EPSCs recorded in DGK $\zeta^{+/+}$  and DGK $\zeta^{-/-}$  Purkinje cells. Calibration: 100 pA, 25 ms. **B**, Amplitudes of PF-EPSCs elicited in DGK $\zeta^{+/+}$  ( $n = 4$ ) or DGK $\zeta^{-/-}$  ( $n = 6$ ) Purkinje cells by PF stimuli of increasing intensity (8, 17, 27, 36, 45, and 54  $\mu$ A). **C**, Amplitudes of mEPSCs in DGK $\zeta^{+/+}$  ( $n = 11$ ) and DGK $\zeta^{-/-}$  ( $n = 10$ ) Purkinje cells, shown as cumulative distributions and bar graphs (inset). Raw exemplar traces are shown at the top. **D**, PPF ratios of PF-EPSCs elicited in DGK $\zeta^{+/+}$  ( $n = 5$ ) or DGK $\zeta^{-/-}$  ( $n = 8$ ) Purkinje cells by a pair of PF stimuli with different intervals (50–250 ms). **E**, Images of distal dendrites of biocytin-labeled Purkinje cells (left) and spine numbers per 10  $\mu$ m dendritic segments (right: DGK $\zeta^{+/+}$ ,  $n = 6$ ; DGK $\zeta^{-/-}$ ,  $n = 7$ ). **F**, Time course of LTD induced by PF $\&\Delta$ V (1 Hz, 300 $\times$ ) in DGK $\zeta^{+/+}$  ( $n = 10$ ) or DGK $\zeta^{-/-}$  ( $n = 7$ ) Purkinje cells. Exemplar traces of PF-EPSCs shown in **F** as well as in the subsequent figures are single (unaveraged) responses before (left) and after (20–30 min, right) stimulation. Calibration: 200 pA, 20 ms. PF-EPSC amplitudes shown in **F** as well as the subsequent figures presenting the time course of PF-EPSCs are normalized to their mean prestimulation level. Error bars indicate SEM.

duced in DGK $\zeta^{-/-}$  mice (K. Kim et al., 2009), suggesting that DGK $\zeta$  plays specific roles in Purkinje cell synapses.

We next examined the involvement of DGK $\zeta$  in LTD. Whereas LTD was induced by pairing PF stimulation with Purkinje cell depolarization at 1 Hz for 300 s (PF $\&\Delta$ V) in Purkinje cells of DGK $\zeta^{+/+}$  mice, LTD was impaired in Purkinje cells of DGK $\zeta^{-/-}$  mice (Fig. 2F). The reduction in PF-EPSC calculated at 20–30 min after PF $\&\Delta$ V was significantly smaller in DGK $\zeta^{-/-}$  mice than in DGK $\zeta^{+/+}$  mice (DGK $\zeta^{+/+}$ ,  $24.3 \pm 3.9\%$ ,  $n = 10$ ; DGK $\zeta^{-/-}$ ,  $-5.77 \pm 4.9\%$ ,  $n = 7$ ;  $p < 0.01$ , Student's  $t$  test). This result indicates that DGK $\zeta$  is involved in cerebellar LTD.

We also tested the involvement of DGK $\zeta$  in another form of synaptic plasticity. LTP at PF-Purkinje cell synapses was triggered by PF stimulation at 1 Hz for 300 s in DGK $\zeta^{+/+}$  slices (Fig. 3A). Consistent with previous reports (Lev-Ram et al., 2002; Coesmans et al., 2004; Belmeguenai and Hansel, 2005), LTP triggered

by a 1 Hz PF stimulation was expressed postsynaptically because PPF ratios were not altered by the stimulation (Fig. 3A). LTP was also observed in DGK $\zeta^{-/-}$  slices, and the potentiation of PF-EPSC in DGK $\zeta^{-/-}$  slices was similar to that in DGK $\zeta^{+/+}$  slices (Fig. 3A; DGK $\zeta^{+/+}$ ,  $32.5 \pm 8.4\%$ ,  $n = 8$ ; DGK $\zeta^{-/-}$ ,  $39.7 \pm 8.8\%$ ,  $n = 6$ ;  $p = 0.572$ , Student's  $t$  test). To further confirm that LTD triggered by 300 s of PF $\&\Delta$ V is altered specifically at PF-Purkinje cell synapses, we tested the effects of a shorter duration (200 s) of pairing PF stimulation with Purkinje cell depolarization on PF-EPSC. With this stimulation protocol, PF-EPSC was neither potentiated nor depressed in DGK $\zeta^{+/+}$  slices (Fig. 3B). Likewise, PF-EPSC was also unaltered in DGK $\zeta^{-/-}$  slices (Fig. 3B). The changes in PF-EPSC that were calculated 20–30 min after this shorter duration of stimulation were not significantly different between DGK $\zeta^{+/+}$  and DGK $\zeta^{-/-}$  slices (DGK $\zeta^{+/+}$ ,  $4.24 \pm 11\%$ ,  $n = 7$ ; DGK $\zeta^{-/-}$ ,  $5.87 \pm 8.8\%$ ,  $n = 6$ ;  $p = 0.912$ , Student's  $t$  test). These results indicate that LTD is impaired specifically at PF-Purkinje cell synapses.

It is well known that LTD requires mGluR activation at PF synapses as well as increases in  $[Ca^{2+}]_i$ , the latter of which results from  $Ca^{2+}$  entry through voltage-dependent  $Ca^{2+}$  channels and  $Ca^{2+}$  release from IP $_3$  receptors (Finch et al., 2012). We tested whether a deficiency of DGK $\zeta$  affects these functions by applying a burst of PF stimulation (100 Hz, 100 ms). The  $[Ca^{2+}]_i$  increase in DGK $\zeta^{-/-}$  Purkinje cells was not significantly different from that in DGK $\zeta^{+/+}$  Purkinje cells (Fig. 3C,E,  $p = 0.4$ , Student's  $t$  test). To investigate the functions of the mGluR and IP $_3$  receptor, CNQX was applied to the extracellular solutions. The increase in  $[Ca^{2+}]_i$  (Fig. 3C,E,  $p = 0.77$ , Student's  $t$  test) and slow EPSCs (Fig. 3D,E,  $p = 0.75$ , Student's  $t$  test) in the presence of CNQX

was also similar between DGK $\zeta^{+/+}$  and DGK $\zeta^{-/-}$  Purkinje cells. These results suggest that a deficiency of DGK $\zeta$  does not affect the signaling upstream of an increase in  $[Ca^{2+}]_i$ .

### PKC $\alpha$ is mislocalized in DGK $\zeta^{-/-}$ Purkinje cells

To elucidate the underlying mechanisms of LTD impairment in DGK $\zeta^{-/-}$  mice, we considered the involvement of the interaction of DGK $\zeta$  with PSD-95 family proteins and PKC $\alpha$  (Luo et al., 2003b; K. Kim et al., 2009) and hypothesized that DGK $\zeta$  promotes the synaptic targeting of PKC $\alpha$  via its interaction with PSD-95 family proteins in Purkinje cells. We confirmed that DGK $\zeta$  indeed interacted with PSD-93, a major PSD-95 family protein expressed in Purkinje cells, in the cerebellum (Fig. 4A). To test our hypothesis, we investigated whether the binding of DGK $\zeta$  to PSD-93 is necessary for LTD induction, by recording LTD in DGK $\zeta^{-/-}$  Purkinje cells expressing wild-type DGK $\zeta$

(DGK $\zeta$ -WT) or a mutant form of DGK $\zeta$  lacking the C-terminal PDZ binding motif (DGK $\zeta$ - $\Delta$ C) that is required for the binding of DGK $\zeta$  to PSD-95 family proteins (K. Kim et al., 2009). Lentiviral vectors expressing DGK $\zeta$ -WT or DGK $\zeta$ - $\Delta$ C fused with GFP were injected into the cerebellum of DGK $\zeta$ <sup>-/-</sup> mice. The expression of DGK $\zeta$  was mainly observed in Purkinje cells (Fig. 4B), as was expected from a report showing that lentiviral vectors driven by the MSCV promoter successfully promoted the expression of molecules in Purkinje cells (Torashima et al., 2006). Expression of DGK $\zeta$ -WT in DGK $\zeta$ <sup>-/-</sup> Purkinje cells restored LTD, confirming that DGK $\zeta$  is required for LTD (Fig. 4C). However, expression of DGK $\zeta$ - $\Delta$ C in DGK $\zeta$ <sup>-/-</sup> Purkinje cells failed to restore LTD (Fig. 4C). The depression of PF-EPSC in cells expressing DGK $\zeta$ - $\Delta$ C was significantly smaller than that in cells expressing DGK $\zeta$ -WT (DGK $\zeta$ -WT, 30 ± 7%, *n* = 6; DGK $\zeta$ - $\Delta$ C, -9.82 ± 12%, *n* = 8; *p* < 0.05, Student's *t* test). These results indicate that the interaction of DGK $\zeta$  with PSD-93 via its PDZ binding motif is required for cerebellar LTD.

By immunoprecipitation analysis using lysates from HEK293T cells expressing DGK $\zeta$  and PKC $\alpha$ , we confirmed that DGK $\zeta$  interacts with PKC $\alpha$  (Fig. 4D). A study previously demonstrated that LTD impairment in PKC $\alpha$ -knocked down Purkinje cells was rescued by the expression of wild-type PKC $\alpha$ , but not by the expression of a PKC $\alpha$  mutant (PKC $\alpha$ -AAAA), in which the unique PDZ-binding motif (QSAV) in the C terminus was replaced with 4 alanine residues (Leitges et al., 2004). Therefore, we tested the interaction of DGK $\zeta$  with PKC $\alpha$ -AAAA. Interestingly, the interaction was severely reduced compared with that between DGK $\zeta$  and wild-type PKC $\alpha$  (Fig. 4D), indicating that the PDZ-binding motif in PKC $\alpha$  is involved in its interaction with DGK $\zeta$ . Together with the study showing the importance of the PDZ-binding motif in PKC $\alpha$  for LTD (Leitges et al., 2004), this result supports the idea that the interaction of PKC $\alpha$  with DGK $\zeta$  via its PDZ-binding motif is required for LTD.

To directly demonstrate that PKC $\alpha$  is mislocalized in DGK $\zeta$ <sup>-/-</sup> Purkinje cells, we next performed immunohistochemical staining of cerebellar slices with antibodies against calbindin and PKC $\alpha$ , and we examined the localization of endogenous PKC $\alpha$  in Purkinje cells of DGK $\zeta$ <sup>+/+</sup> and DGK $\zeta$ <sup>-/-</sup> slices. In DGK $\zeta$ <sup>+/+</sup> slices, immunosignals of PKC $\alpha$  were detected equally in both Purkinje cell soma and the molecular layer, the latter of which is mostly occupied by Purkinje cell dendrites (Fig. 5A). The ratio of PKC $\alpha$  staining in the molecular layer to that in soma was 1.13 ± 0.1 (Fig. 5B), indicating the ubiquitous distribution of PKC $\alpha$  throughout DGK $\zeta$ <sup>+/+</sup> Purkinje cells. In contrast, PKC $\alpha$  staining in Purkinje cell soma was enhanced in DGK $\zeta$ <sup>-/-</sup> slices (Fig. 5A). The ratio of PKC $\alpha$  staining in the molecular layer to that in soma in DGK $\zeta$ <sup>-/-</sup> slices was significantly decreased com-

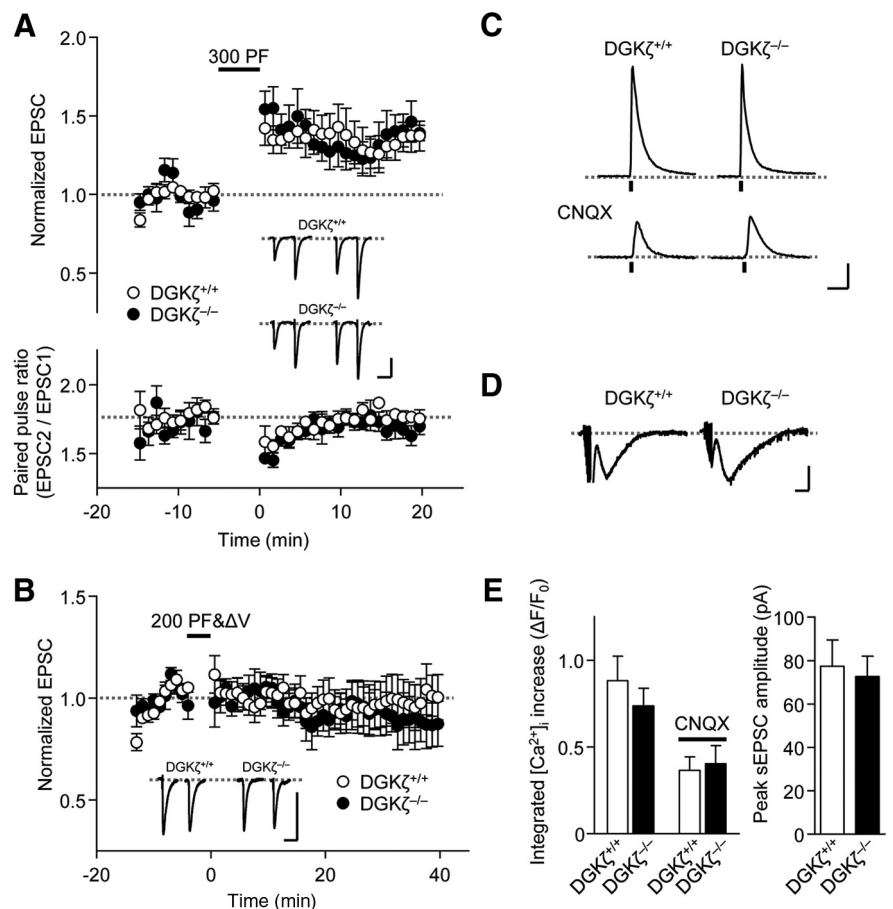


**Figure 3.** LTP at PF-Purkinje cell synapses is unaffected in DGK $\zeta$ <sup>-/-</sup> Purkinje cells. **A**, Time course of LTP induced by PF stimuli (1 Hz, 300×) in DGK $\zeta$ <sup>+/+</sup> (*n* = 7) and DGK $\zeta$ <sup>-/-</sup> (*n* = 5) Purkinje cells. Bottom, Accompanying PPF ratios of PF-EPSC elicited by a pair of PF stimuli with a 100 ms interval. **B**, Time course of changes in PF-EPSC amplitudes before and after a pairing stimulation of PF with Purkinje cell depolarization (1 Hz, 200×) recorded from DGK $\zeta$ <sup>+/+</sup> (*n* = 7) and DGK $\zeta$ <sup>-/-</sup> (*n* = 6) Purkinje cells. **C**, Changes in OGB1 fluorescence ( $\Delta F/F_0$ ) measured in DGK $\zeta$ <sup>+/+</sup> or DGK $\zeta$ <sup>-/-</sup> Purkinje cell dendrites in the absence or presence of CNQX (25  $\mu$ M) upon burst PF stimulation at 100 Hz for 100 ms. Calibration: 0.5  $\Delta F/F_0$ , 1 s. **D**, Representative traces of slow EPSC elicited by burst PF stimulation and recorded from DGK $\zeta$ <sup>+/+</sup> or DGK $\zeta$ <sup>-/-</sup> Purkinje cells in the presence of CNQX. Calibration: 50 pA, 200 ms. **E**, Summary of OGB1 fluorescence changes ( $\Delta F/F_0$ ) and peak amplitudes of slow EPSCs (*n* = 10, *n* = 16). Error bars indicate SEM.

pared with the ratio in DGK $\zeta$ <sup>+/+</sup> slices (Fig. 5B, *p* < 0.01, Student's *t* test). Because the total amount of endogenous PKC $\alpha$  was not altered by the loss of DGK $\zeta$  (Fig. 5C), an alteration of PKC $\alpha$  distribution is not due to an increase or decrease in the total amount of PKC $\alpha$  in Purkinje cells. Furthermore, we measured the amount of PKC $\alpha$  in the fractionated components of the cerebellum: cytosolic fractions (S2) and crude synaptosomal fractions (P2). The P2 fraction was confirmed by the concentration of synaptic proteins, namely, the GluA2 subunit of the AMPAR, PICK1, and synapsin (Fig. 5D). In the DGK $\zeta$ <sup>-/-</sup> cerebellum, the amount of PKC $\alpha$  in P2 fractions was reduced compared with that in the DGK $\zeta$ <sup>+/+</sup> cerebellum, whereas the amount of the GluA2 and synapsin was similar to those in the DGK $\zeta$ <sup>+/+</sup> cerebellum (Fig. 5D). To quantify the amount of various proteins in the fractions, we calculated the ratio of band intensities in the P2 fractions to those in the S2 fractions (Fig. 5E). The ratio of PKC $\alpha$  was significantly lower in the DGK $\zeta$ <sup>-/-</sup> cerebellum than that in the DGK $\zeta$ <sup>+/+</sup> cerebellum, whereas ratios for GluA2 and synapsin were comparable between the DGK $\zeta$ <sup>+/+</sup> and DGK $\zeta$ <sup>-/-</sup> cerebellum. These results indicate that a lower amount of PKC $\alpha$  is localized in synapses and dendrites of DGK $\zeta$ <sup>-/-</sup> Purkinje cells than DGK $\zeta$ <sup>+/+</sup> Purkinje cells.

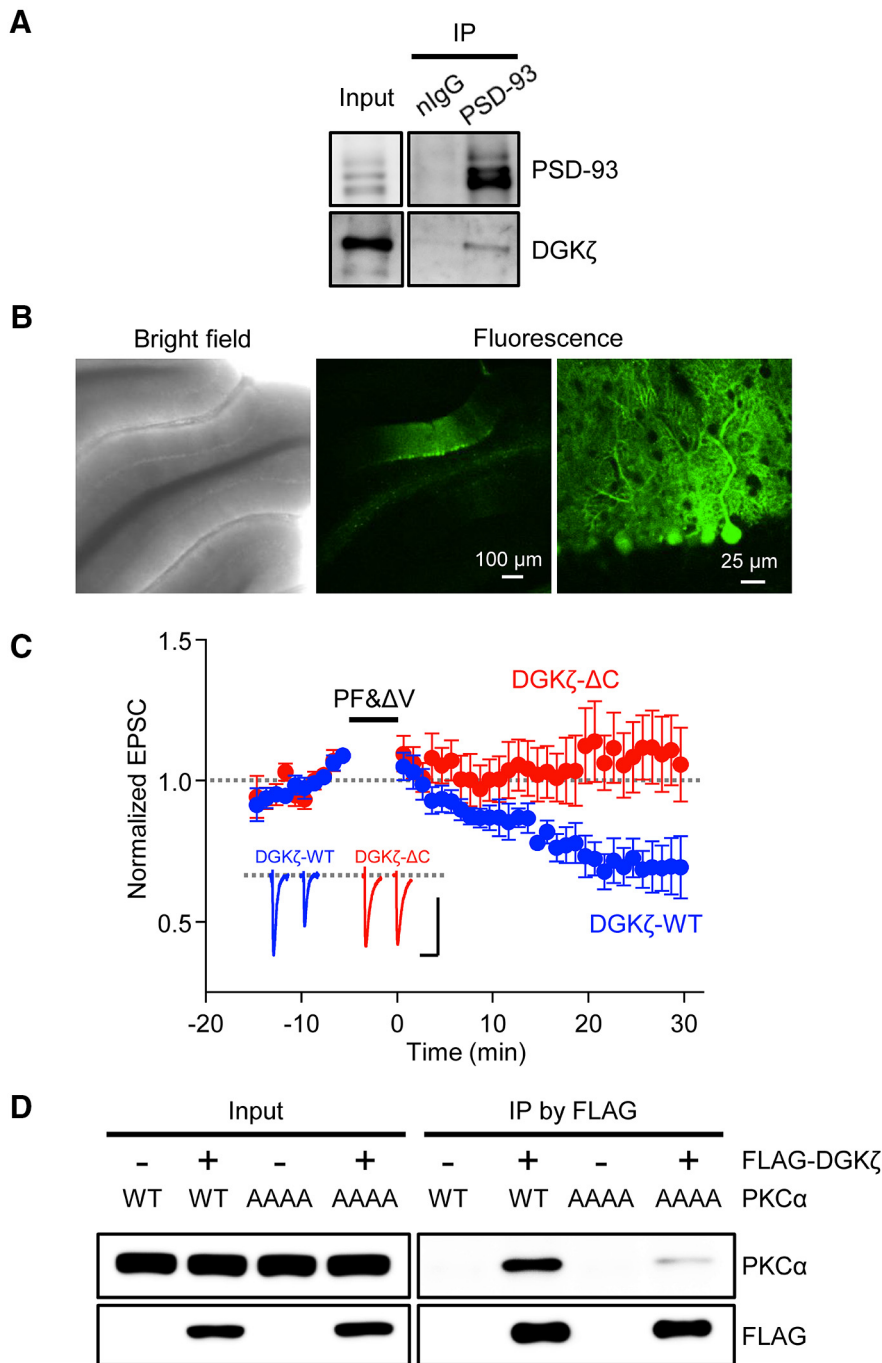


**Figure 4.** Binding of DGK $\zeta$  with PSD-95 family proteins is required for LTD. **A**, Immunoblot of coimmunoprecipitated DGK $\zeta$  and precipitated PSD-93 in DGK $\zeta^{+/+}$  cerebellum. Normal IgG (nlGg) was used as a control. **B**, Bright-field and fluorescence images of live cerebellar slices obtained from a DGK $\zeta^{-/-}$  mouse injected with a lentiviral vector expressing GFP-DGK $\zeta$ -WT. **C**, Time course of LTD induced by PF& $\Delta$ V (1 Hz, 300 $\times$ ) in Purkinje cells expressing DGK $\zeta$ -WT (blue circles,  $n = 6$ ) and DGK $\zeta$ - $\Delta$ C (red circles,  $n = 8$ ). Error bars indicate SEM. **D**, Immunoblot of coimmunoprecipitated PKC $\alpha$ -WT or PKC $\alpha$ -AAAA mutant, and immunoprecipitated FLAG-DGK $\zeta$  in HEK293T cells expressing FLAG-DGK $\zeta$  together with either PKC $\alpha$ -WT or PKC $\alpha$ -AAAA.

We also tested whether PKC $\alpha$  activity is reduced in DGK $\zeta^{-/-}$  Purkinje cell dendrites. Previous studies suggested that PKC $\alpha$  activation reduces the dendritic branching of Purkinje cells (Gundlfinger et al., 2003). We thus examined the dendritic branching pattern of biocytin-labeled Purkinje cells in DGK $\zeta^{+/+}$  and DGK $\zeta^{-/-}$  mice (Fig. 5F). Sholl analysis demonstrated that dendritic branching was enhanced in distal dendrites of DGK $\zeta^{-/-}$  Purkinje cells compared with DGK $\zeta^{+/+}$  Purkinje cells (Fig. 5G, whole dendrites,  $p < 0.01$ , two-way ANOVA; dendrites

at a distance of 210–250  $\mu$ m,  $p < 0.05$ , Student's  $t$  test). This result suggests that PKC $\alpha$  activity is reduced in Purkinje cell dendrites of DGK $\zeta^{-/-}$  mice. Thus, deletion of DGK $\zeta$  results in less PKC $\alpha$  localization in synapses as well as dendrites of Purkinje cells, and such mislocalization of PKC $\alpha$  likely leads to the reduced activity of PKC $\alpha$  around synapses and consequently to LTD impairment.

#### DGK $\zeta$ kinase activity is required for LTD induction

Our results so far suggest that the PDZ binding motif-dependent anchoring function of DGK $\zeta$  is important for the proper localization of PKC $\alpha$  and cerebellar LTD. We next examined whether the kinase function of DGK $\zeta$ , which leads to the metabolism of DAG, is also involved in LTD. For this purpose, we performed rescue experiments using AAV vectors expressing wild-type (DGK $\zeta$ -WT) or a kinase-dead mutant of DGK $\zeta$  (DGK $\zeta$ -KD) fused with GFP, as well as GFP alone. With our experimental conditions, GFP fluorescence was observed almost exclusively in Purkinje cells (Fig. 6A) (Y. Kim et al., 2015). Expression of DGK $\zeta$ -WT in DGK $\zeta^{-/-}$  Purkinje cells restored LTD (Fig. 6B;  $29.9 \pm 4.9\%$ ,  $n = 5$ ), as seen in the rescue experiments with lentiviral vectors. In contrast, expression of DGK $\zeta$ -KD as well as GFP alone failed to restore LTD (Fig. 6B; DGK $\zeta$ -KD,  $-6.93 \pm 8.6\%$ ,  $n = 8$ ; GFP,  $-5.03 \pm 8.9\%$ ,  $n = 6$ ). ANOVA confirmed the significance of the difference ( $p < 0.05$ ), and multiple comparison by the Tukey test confirmed that LTD in cells expressing DGK $\zeta$ -KD was significantly smaller than that in cells expressing DGK $\zeta$ -WT ( $p < 0.05$ ) but was not significantly different from LTD in cells expressing GFP alone ( $p = 0.998$ ). We also analyzed alterations of PKC $\alpha$  distribution by immunohistochemical staining of cerebellar slices expressing DGK $\zeta$ -WT, DGK $\zeta$ -KD, or GFP alone, with an antibody against PKC $\alpha$  (Fig. 6C). The ratio of PKC $\alpha$  staining in the molecular layer to that in soma in DGK $\zeta^{-/-}$  slices expressing DGK $\zeta$ -WT or DGK $\zeta$ -KD was both significantly increased compared with the ratio in slices expressing GFP alone (DGK $\zeta$ -WT,  $0.75 \pm 0.03$ ,  $n = 19$ ; DGK $\zeta$ -KD,  $0.66 \pm 0.02$ ,  $n = 23$ ; GFP,  $0.59 \pm 0.02$ ,  $n = 22$ ;  $p < 0.05$ , Bonferroni test), suggesting that the failure to restore LTD in cells expressing DGK $\zeta$ -KD is not due to the mislocalization of PKC $\alpha$ . These results indicate that not only the anchoring function, but also the kinase activity, of DGK $\zeta$  is required for LTD. DGK $\zeta$ -KD is able to anchor PKC $\alpha$  to synapses but does not metabolize DAG, so that PKC $\alpha$  activity may be enhanced at the synapses of Purkinje cells expressing DGK $\zeta$ -KD. However, it is unlikely that such enhanced

PKC $\alpha$  activity triggers LTD and inhibits the further induction of LTD because the PF-EPSC amplitude at the basal level was not depressed, and presynaptic glutamate release was unaltered in cells expressing DGK $\zeta$ -KD (Fig. 6*D,E*; PF-EPSC amplitude,  $p = 0.717$ ; PPF,  $p = 0.232$ , two-way ANOVA).

DGK $\zeta$  not only metabolizes DAG, but also produces PA. One possibility by which PA may be involved in LTD is by activation of the MAPK pathway (Rizzo et al., 1999, 2000). However, the level of MAPK activation in DGK $\zeta^{-/-}$  cerebellar slices was equivalent to that in DGK $\zeta^{+/+}$  slices, with or without chemical LTD stimulation (Fig. 6*F*), suggesting that PA produced by DGK $\zeta$  is not the major pathway of MAPK activation during LTD. Therefore, the kinase activity of DGK $\zeta$  appears to be required for reducing DAG signaling, rather than for activating PA signaling, during LTD.

#### Activity-dependent dissociation of PKC $\alpha$ from DGK $\zeta$ is required for LTD

A previous study proposed a model of the reciprocal regulation of DGK $\zeta$  by PKC $\alpha$  (Luo et al., 2003b): activated PKC $\alpha$  phosphorylates DGK $\zeta$ , the phosphorylation of DGK $\zeta$  results in the dissociation of PKC $\alpha$  from DGK $\zeta$ , and the dissociation allows PKC $\alpha$  to remain active without being suppressed by DGK $\zeta$ . Because PKC $\alpha$  activation is critical for LTD, it is possible that such reciprocal regulation occurs during LTD. We tested this possibility by two experiments. First, we performed immunoprecipitation analysis using lysates from cerebellar slices to examine the interaction between PKC $\alpha$  and DGK $\zeta$  in the cerebellum. For this analysis, chemical LTD stimulation with K-glu was used to induce LTD in cerebellar slices. We previously showed that K-glu treatment for 5 min indeed induced LTD (Tanaka and Augustine, 2008; Yamamoto et al., 2012), and further confirmed that the preincubation of slices with K-glu occluded PF& $\Delta$ V-evoked LTD because LTD was not induced in slices pre-treated with K-glu for 5 min (Fig. 7*A*,  $-8.93 \pm 9.5\%$ ,  $n = 4$ ;  $p < 0.01$  compared with LTD in DGK $\zeta^{+/+}$  Purkinje cells shown in Fig. 2*F*, Student's  $t$  test). In the control cerebellar slices that were incubated in normal ACSF, PKC $\alpha$  was immunoprecipitated by the PKC $\alpha$  antibody. We then found that a substantial amount of DGK $\zeta$  was coimmunoprecipitated by this antibody in the control slices, whereas much less was immunoprecipitated by normal IgG (Fig. 7*B*), indicating the interaction of PKC $\alpha$  with DGK $\zeta$  in the cerebellum. Compared with the control slices, the amounts of coimmunoprecipitated DGK $\zeta$  were reduced following treatment of the slices with chemical LTD stimulation with K-glu (Fig. 7*B*). To quantify the interaction of

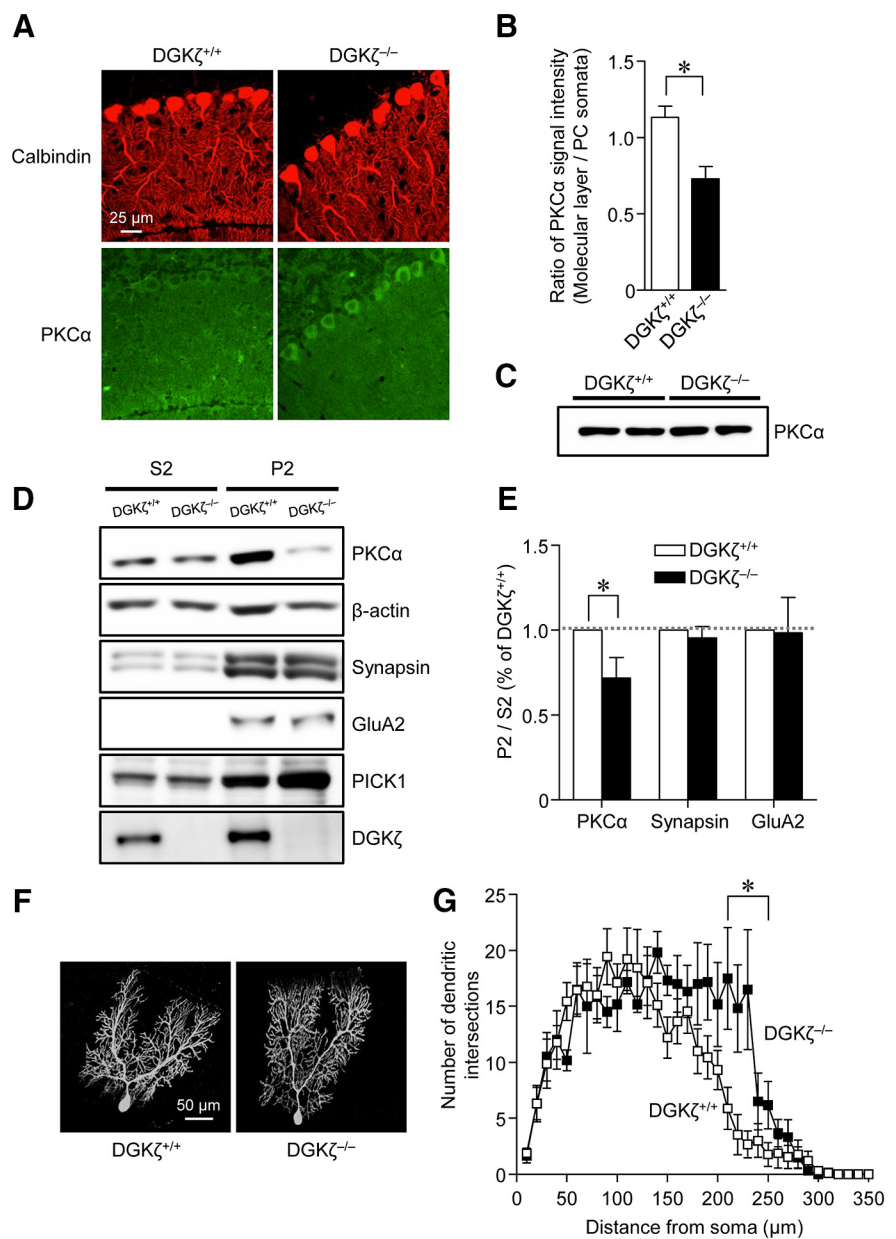


**Figure 5.** Reduced dendritic and synaptic localization of PKC $\alpha$  in DGK $\zeta^{-/-}$  Purkinje cells. **A**, Images of DGK $\zeta^{+/+}$  and DGK $\zeta^{-/-}$  cerebellar slices double stained with antibodies against calbindin and PKC $\alpha$ . **B**, The ratio of the PKC $\alpha$  signal in the molecular layer to that in the soma (DGK $\zeta^{+/+}$ ,  $n = 24$ ; DGK $\zeta^{-/-}$ ,  $n = 24$ ). **C**, Immunoblotting using an antibody against PKC $\alpha$  in DGK $\zeta^{+/+}$  and DGK $\zeta^{-/-}$  cerebellar lysates. **D**, Immunoblotting using antibodies against PKC $\alpha$ ,  $\beta$ -actin, synapsin, GluA2, PICK1, and DGK $\zeta$  in S2 and P2 fractions obtained from DGK $\zeta^{+/+}$  or DGK $\zeta^{-/-}$  cerebellum. **E**, Ratios of PKC $\alpha$ , synapsin, and GluA2 signals in P2 fractions to those in S2 fractions (DGK $\zeta^{+/+}$ ,  $n = 9$ ; DGK $\zeta^{-/-}$ ,  $n = 9$ ). Ratios are normalized to those of DGK $\zeta^{+/+}$  cerebellum. **B**, **E**, Statistically significant difference between DGK $\zeta^{+/+}$  and DGK $\zeta^{-/-}$  mice: **B**,  $*p < 0.01$  (Student's  $t$  test); **E**,  $*p < 0.05$  (Student's  $t$  test). **F**, Images of biocytin-labeled Purkinje cells of DGK $\zeta^{+/+}$  and DGK $\zeta^{-/-}$  mice. **G**, Sholl analysis of the number of dendritic intersections in DGK $\zeta^{+/+}$  ( $n = 9$ ) and DGK $\zeta^{-/-}$  ( $n = 6$ ) Purkinje cells. \*Statistically significant difference between DGK $\zeta^{+/+}$  and DGK $\zeta^{-/-}$  Purkinje cells ( $p < 0.05$ , Student's  $t$  test). Open and filled symbols represent results obtained from DGK $\zeta^{+/+}$  and DGK $\zeta^{-/-}$  Purkinje cells, respectively. In all graphs, error bars indicate SEM.

DGK $\zeta$  with PKC $\alpha$ , the ratio of band intensities of DGK $\zeta$  and PKC $\alpha$  was calculated. We found that the ratio was significantly smaller in K-glu-treated samples than the control samples (Fig. 7*C*,  $p < 0.05$ , Student's  $t$  test). These results indicate that PKC $\alpha$  is dissociated from DGK $\zeta$  after LTD stimulation.

Second, to test whether the reciprocal regulation of DGK $\zeta$  by PKC $\alpha$  is necessary for LTD, we performed rescue experiments using a mutant form of DGK $\zeta$ , in which four serine residues were replaced



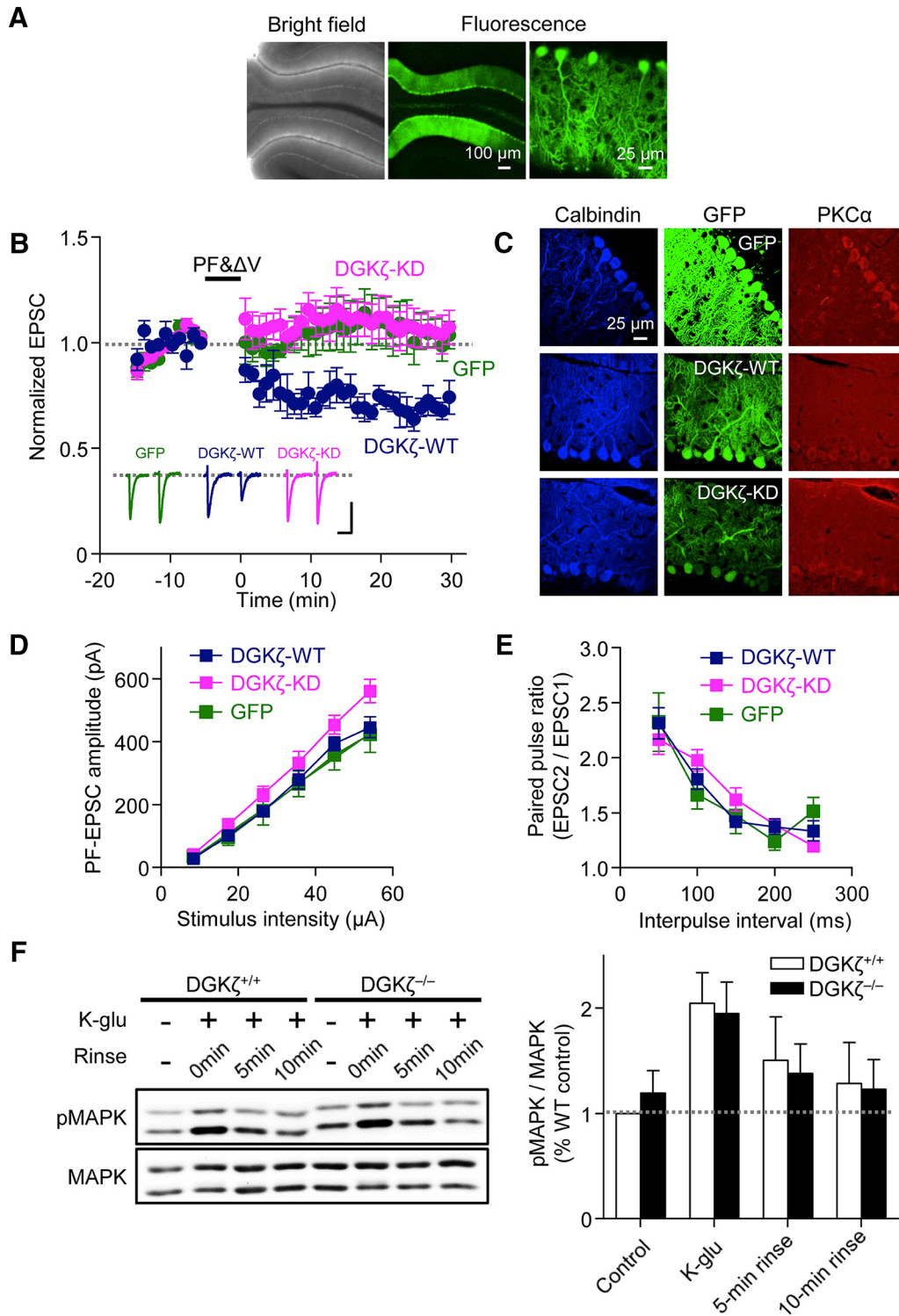


**Figure 6.** Kinase activity of DGK $\zeta$  is required for LTD. **A**, Bright-field and fluorescence images of live cerebellar slices obtained from a DGK $\zeta^{-/-}$  mouse injected with an AAV vector expressing GFP-DGK $\zeta$ -WT. **B**, Time course of LTD induced by PF $\Delta$ V (1 Hz, 300 $\times$ ) in Purkinje cells expressing DGK $\zeta$ -WT ( $n = 5$ ), DGK $\zeta$ -KD ( $n = 8$ ), or GFP alone ( $n = 6$ ). **C**, Images of DGK $\zeta^{-/-}$  cerebellar slices expressing GFP-DGK $\zeta$ -WT, GFP-DGK $\zeta$ -KD, or GFP alone. Slices were double stained with antibodies against calbindin and PKC $\alpha$ . **D**, Amplitudes of PF-EPSCs elicited in Purkinje cells expressing DGK $\zeta$ -WT ( $n = 8$ ), DGK $\zeta$ -KD ( $n = 10$ ), or GFP alone ( $n = 7$ ) by PF stimuli of increasing intensity (8, 17, 27, 36, 45, and 54  $\mu$ A). **E**, PPF ratios of PF-EPSCs elicited in Purkinje cells expressing DGK $\zeta$ -WT ( $n = 11$ ), DGK $\zeta$ -KD ( $n = 11$ ), or GFP alone ( $n = 9$ ) by a pair of PF stimuli with different intervals (50–250 ms). **B**, **D**, **E**, Dark blue, magenta, and green symbols represent results obtained from Purkinje cells expressing DGK $\zeta$ -WT, DGK $\zeta$ -KD, and GFP alone, respectively. **F**, Immunoblots detecting MAPK and phosphorylated MAPK (pMAPK) in DGK $\zeta^{+/+}$  and DGK $\zeta^{-/-}$  cerebellar slices that were lysed after incubating in normal ACSF (control), or immediately (K-glu), 5 min (5 min rinse), or 10 min (10 min rinse) after K-glu stimulation. Right, Ratios of the pMAPK signal to the MAPK signal normalized to the ratio in control DGK $\zeta^{+/+}$  slices (DGK $\zeta^{+/+}$ ,  $n = 4$ ; DGK $\zeta^{-/-}$ ,  $n = 4$ ). Error bars indicate SEM.

with asparagine residues (DGK $\zeta$ -SN). It was reported that DGK $\zeta$ -SN maintained its kinase activity and that the interaction of PKC $\alpha$  with DGK $\zeta$ -SN was not affected by the activation or inhibition of PKC $\alpha$  (Luo et al., 2003b), so that DGK $\zeta$ -SN was considered as a mutant that does not receive reciprocal regulation by PKC $\alpha$ . As with DGK $\zeta$ -WT and DGK $\zeta$ -KD, an AAV vector expressing DGK $\zeta$ -SN was injected into the DGK $\zeta^{-/-}$  cerebellum. We found that the expression of DGK $\zeta$ -SN in DGK $\zeta^{-/-}$  Purkinje cells failed to restore LTD (Fig. 7D). The depression of PF-EPSC in cells expressing DGK $\zeta$ -SN ( $-6.8 \pm 7.6\%$ ,  $n = 7$ ) was significantly smaller than that in cells expressing DGK $\zeta$ -WT ( $p < 0.05$ , Tukey test). Similar to the case of DGK $\zeta$ -KD, changes of PKC $\alpha$  distribution in DGK $\zeta^{-/-}$  slices expressing DGK $\zeta$ -SN were analyzed (Fig. 7E). The ratio of PKC $\alpha$  staining in the molecular layer to that in soma in DGK $\zeta^{-/-}$  slices expressing DGK $\zeta$ -SN ( $0.71 \pm 0.02$ ,  $n = 19$ ) was significantly increased compared with the ratio in DGK $\zeta^{-/-}$  slices expressing GFP alone ( $p < 0.05$ , Bonferroni test), suggesting that the failure to restore LTD by DGK $\zeta$ -SN expression is not due to the mislocalization of PKC $\alpha$ . Finally, because the failure of DGK $\zeta$ -SN to restore LTD may be overcome by a stimulation that strongly activates PKC $\alpha$ , even without the reciprocal regulation of DGK $\zeta$ -SN by PKC $\alpha$ , we tested whether a longer duration (500 s) of pairing PF stimulation with Purkinje cell depolarization (500 PF& $\Delta$ V) could trigger LTD in DGK $\zeta^{-/-}$  Purkinje cells expressing DGK $\zeta$ -SN. Although LTD was not clearly induced by 500 PF& $\Delta$ V, there was a tendency of slight depression (Fig. 7D;  $12.3 \pm 4.2\%$ ,  $n = 6$ ). No significant difference was detected upon comparison with both cases, in which a 300 s duration of PF& $\Delta$ V induced or did not induce LTD in cells expressing DGK $\zeta$ -WT ( $p = 0.17$ , Tukey test) or DGK $\zeta$ -SN ( $p = 0.093$ , Tukey test), respectively. Thus, small amounts of LTD may have been induced by stronger PKC $\alpha$  activation following 500 PF& $\Delta$ V in DGK $\zeta^{-/-}$  Purkinje cells expressing DGK $\zeta$ -SN. Together with the results of immunoprecipitation analysis, we conclude that the reciprocal regulation of DGK $\zeta$  by PKC $\alpha$ , which presumably leads to the dissociation of PKC $\alpha$  from DGK $\zeta$  and consequently to further PKC $\alpha$  activation, is required for LTD induction.

## Discussion

PKC has been established to be necessary and even sufficient for cerebellar LTD (Linden and Connor, 1991; Hartell, 1994;

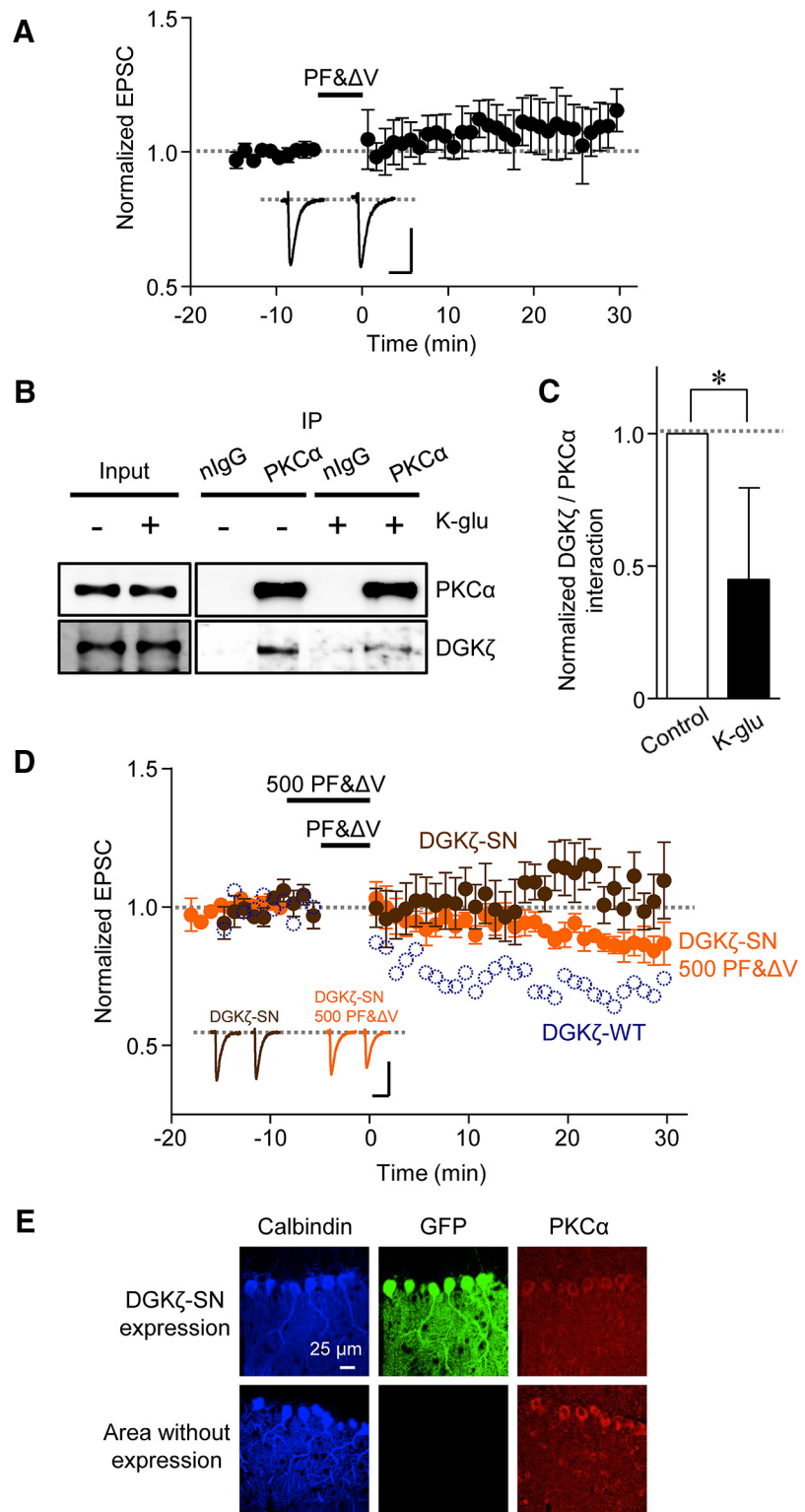


**Figure 7.** Activity-dependent dissociation of DGK $\zeta$  and PKC $\alpha$  is necessary for LTD. **A**, Inhibition of PF& $\Delta$ V-evoked LTD by preincubation of DGK $\zeta^{+/+}$  cerebellar slices with K-glu for 5 min ( $n = 4$ ). PF& $\Delta$ V stimulation was applied at  $\sim 30$  min after the end of K-glu treatment. **B**, Immunoblotting of coimmunoprecipitated DGK $\zeta$  and precipitated PKC $\alpha$  in DGK $\zeta^{+/+}$  cerebellar slices treated with or without K-glu. Normal IgG (nlgG) was used as a control. **C**, Ratio of the signal of coimmunoprecipitated DGK $\zeta$  to the signal of precipitated PKC $\alpha$  ( $n = 5$ ). \*Statistically significant difference ( $p < 0.05$ , Student's  $t$  test). **D**, Time course of LTD induced by PF& $\Delta$ V (1 Hz, 300  $\times$ , brown circles,  $n = 7$ ) or 500 PF& $\Delta$ V (1 Hz, 500 times, orange circles,  $n = 6$ ) in Purkinje cells expressing DGK $\zeta$ -SN. For comparison, the time course of LTD in Purkinje cells expressing DGK $\zeta$ -WT shown in Figure 6B is overlaid (dark blue dotted circles). **E**, Images of a cerebellar slice from a DGK $\zeta^{-/-}$  mouse expressing GFP-DGK $\zeta$ -SN. The slice was double stained with antibodies against calbindin and PKC $\alpha$ . For comparison, images of an area of the same slice, in which GFP expression was not observed, are also shown.

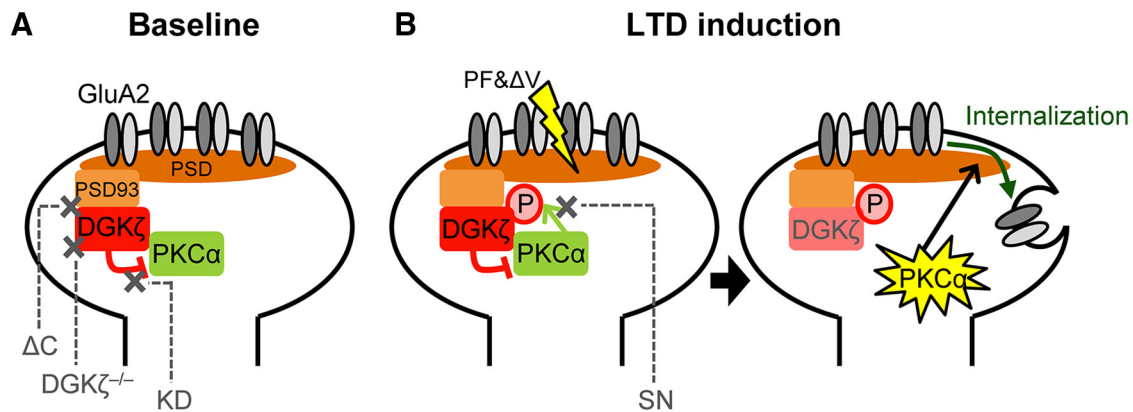


**Figure 8.** Proposed model of the role of DGK $\zeta$  in the regulation of PKC $\alpha$  activity and LTD at baseline (**A**) and after LTD induction (**B**). The affected proteins/functions in DGK $\zeta^{-/-}$  Purkinje cells, with or without the expression of mutant forms of DGK $\zeta$ , namely, DGK $\zeta$ - $\Delta$ C ( $\Delta$ C), DGK $\zeta$ -KD (KD), or DGK $\zeta$ -SN (SN), are indicated by crosses.

De Zeeuw et al., 1998; Endo and Launey, 2003; Kondo et al., 2005); hence, the precise regulation of PKC is critical for synaptic functions. We investigated the role of DGK $\zeta$ , which was shown to physically and functionally interact with PKC $\alpha$ , in the regulation of LTD. The present study demonstrated several results indicating that DGK $\zeta$  indeed regulates PKC $\alpha$  and consequently LTD: (1) LTD is impaired in DGK $\zeta^{-/-}$  Purkinje cells; (2) PKC $\alpha$  is less localized in the dendrites and synapses of DGK $\zeta^{-/-}$  Purkinje cells compared with DGK $\zeta^{+/+}$  Purkinje cells, and targeting of DGK $\zeta$  to synapses is required for LTD; (3) the kinase activity of DGK $\zeta$  is involved in LTD; and (4) the binding between PKC $\alpha$  and DGK $\zeta$  is reduced upon LTD stimulation, and the inverse regulation from PKC $\alpha$  to DGK $\zeta$ , which presumably leads to the dissociation of PKC $\alpha$  from DGK $\zeta$ , is required for LTD. Together, our study revealed the importance of DGK $\zeta$  in cerebellar LTD, and further presented the underlying mechanisms of the regulation by DGK $\zeta$  of the localization and activity of PKC $\alpha$  that is required for LTD.

#### Mutual regulation of PKC $\alpha$ and DGK $\zeta$ is required for cerebellar LTD

Based on the results of this study, we propose a model as to how DGK $\zeta$  controls PKC $\alpha$  in terms of synaptic regulation in cerebellar Purkinje cells (Fig. 8). Results showing the mislocalization of PKC $\alpha$  in DGK $\zeta^{-/-}$  Purkinje cells indicate that DGK $\zeta$  works to place PKC $\alpha$  in its correct position. Because DGK $\zeta$  can interact with PKC $\alpha$  and the targeting of DGK $\zeta$  to synapses is required for LTD, DGK $\zeta$ -dependent anchoring of PKC $\alpha$  at synapses is likely to be a function of DGK $\zeta$  that is required for LTD. In addition to its anchoring function, the kinase activity of DGK $\zeta$  is also required for LTD, based on the results showing that DGK $\zeta$ -KD could not restore LTD. Although it is not entirely clear as to how the kinase activity of DGK $\zeta$  is involved in LTD, considering that DGK $\zeta$  metabolizes DAG, leading to a decrease in PKC $\alpha$  activity, and that an increase rather than a decrease in PKC $\alpha$  activity mediates LTD, one possibility is that the reduction of PKC $\alpha$  activity by DGK $\zeta$  works at the basal state. Thus, the anchoring function, as well as the kinase activity of DGK $\zeta$  for PKC $\alpha$ , appears to prepare synapses to respond to the synaptic stimulation that triggers LTD. Furthermore, our results using DGK $\zeta$ -SN indicate that the functions of DGK $\zeta$  in anchoring PKC $\alpha$  to synapses and in reducing PKC $\alpha$  activity are not sufficient, and that the inverse regulation from PKC $\alpha$  to DGK $\zeta$  and the following dissociation of PKC $\alpha$  are required for LTD. Indeed, our immunoprecipitation analysis showed that PKC $\alpha$  was dissociated from DGK $\zeta$  upon

LTD stimulation. The requirement of this inverse regulation also supports the idea that the kinase activity of DGK $\zeta$  is required for reducing PKC $\alpha$  activity at the basal state. Thus, PKC $\alpha$  activity is maintained at a reduced level around synapses by DGK $\zeta$  in the basal state (Fig. 8A), but synaptic stimulation triggering LTD activates PKC $\alpha$  through Ca $^{2+}$  and DAG production, and the activated PKC $\alpha$  phosphorylates DGK $\zeta$  and is released from DGK $\zeta$ , so that PKC $\alpha$  can effectively trigger LTD by enhancing AMPAR internalization (Fig. 8B).

Unlike other isoforms of PKC, PKC $\alpha$  has a unique PDZ ligand motif in its C terminus, and this PDZ ligand motif is critical for the function of PKC $\alpha$  in LTD (Leitges et al., 2004). The PDZ ligand motif in PKC $\alpha$  is responsible for its interaction with PICK1 (Staudinger et al., 1997). Furthermore, the interaction of PICK1 with GluA2 AMPARs after PKC-dependent GluA2 phosphorylation is required for the internalization of AMPARs during LTD (Steinberg et al., 2006). These reports suggest that the requirement of the PDZ ligand motif in PKC $\alpha$  for LTD arises from its interaction with PICK1 (Leitges et al., 2004). In the present study, we showed that the interaction between DGK $\zeta$  and PKC $\alpha$  relies on the PDZ ligand motif in PKC $\alpha$  (Fig. 4C), raising the possibility that this motif is critical for LTD, also because of its interaction with DGK $\zeta$ . Because PICK1 interacts with PKC $\alpha$  only in the activated state (Perez et al., 2001), whereas DGK $\zeta$  interacts with PKC $\alpha$  in the inactivated state (Luo et al., 2003b), these two interacting partners of PKC $\alpha$  act cooperatively: DGK $\zeta$  interacts with PKC $\alpha$  at the basal level to control the localization of and to reduce the activity of PKC $\alpha$ , but upon LTD stimulation, PKC $\alpha$  is released from DGK $\zeta$  and PICK1 interacts with PKC $\alpha$  to perform further reactions required for LTD. This idea could be verified by investigating the presence of three molecules in the same synaptic signaling clusters and analyzing the mechanisms causing the switch of PKC $\alpha$ -interacting partners during LTD. The former would be supported by our results showing that all three proteins were concentrated in the P2 fraction of DGK $\zeta^{+/+}$  cerebella (Fig. 5D). The mechanisms involved in the switch of interaction partners are not clear but may involve an increased binding affinity of PKC $\alpha$  with an active conformation to PICK1 (Leonard et al., 2011; Erlendsson et al., 2014), and a decreased binding affinity of PKC $\alpha$  to phosphorylated DGK $\zeta$ .

Our immunoblotting analysis using synaptosomes demonstrated that the synaptic localization of PKC $\alpha$  relies on DGK $\zeta$ . In addition, our immunohistochemical analysis showing less PKC $\alpha$  localization at dendrites in DGK $\zeta^{-/-}$  Purkinje cells compared with DGK $\zeta^{+/+}$  Purkinje cells indicated that the dendritic local-

ization of PKC $\alpha$  is also affected by DGK $\zeta$ . Because PSD-93 is distributed throughout soma and dendrites of Purkinje cells (Brenman et al., 1996; McGee et al., 2001), DGK $\zeta$  may also interact with PSD-93 in soma or dendrites. Alternatively, many DGK $\zeta$ -interacting partners have been identified (Rincón et al., 2012), and these proteins may determine the dendritic localization of DGK $\zeta$  and PKC $\alpha$ . Studies regarding DGK $\zeta$ -interacting partners support the concept that DGK $\zeta$  works as a component in protein complexes, where lipid-metabolizing enzymes and lipid effectors act together to coordinate lipid signaling in a local area (Rincón et al., 2012). The present result showing that DGK $\zeta$  functions to target and regulate PKC $\alpha$  around synapses for cerebellar LTD is in line with this concept.

### Regulation of synaptic plasticity by DGK $\zeta$ in Purkinje cells and hippocampal pyramidal cells

It has been shown previously that DGK $\zeta$  regulates synaptic plasticity in Schaffer collateral-CA1 pyramidal (SC-CA1) synapses in the hippocampus (Seo et al., 2012). In these synapses of DGK $\zeta^{-/-}$  mice, LTP is enhanced but LTD is attenuated because of an abnormally increased level of DAG and the subsequent enhancement of PKC activity. In contrast, our results showed that LTD is impaired in PF-Purkinje cell synapses of DGK $\zeta^{-/-}$ , and yet LTP is intact, indicating that DGK $\zeta$  specifically contributes to LTD. Many factors may be involved in creating the differences of DGK $\zeta$  function in the regulation of synaptic plasticity between these two types of synapses. One factor may be the way in which DAG-related molecules, phospholipase C (PLC) and PKC, are involved in synaptic plasticity. Given that inhibitors of PLC or PKC did not affect LTP and LTD in wild-type SC-CA1 synapses (Seo et al., 2012), PLC and PKC in SC-CA1 synapses can be considered as “modulators,” which are molecules modulating the ability to trigger synaptic plasticity or playing a permissive role (Citri and Malenka, 2008). On the other hand, PLC and PKC working in cerebellar LTD are considered as “mediators,” which are directly responsible for triggering synaptic plasticity (Citri and Malenka, 2008). DGK $\zeta$ -regulating modulators may arrange overall synaptic conditions in SC-CA1 synapses, whereas DGK $\zeta$ -regulating mediators may directly regulate LTD of PF-Purkinje cell synapses. Even though the machinery involving DGK $\zeta$  is different, DGK $\zeta$  deficiency affects synaptic plasticity in both types of synapses, suggesting the general importance of DAG-related molecules and their regulation by DGK $\zeta$  for coordinating synaptic plasticity.

### Balance between positive and negative regulators working for cerebellar LTD

Synaptic plasticity is generally triggered by the strong stimulation of synapses, in which many signaling molecules are involved and activated. LTD at PF-Purkinje cell synapses in the cerebellum is mediated by a positive feedback kinase loop (Kuroda et al., 2001; Tanaka and Augustine, 2008; Le et al., 2010), which is an effective mechanism to enhance the amplitude or timing of activation upon stimulation, but also might be problematic for the control of specificity. Therefore, negative regulators, such as phosphatases, are included in the theoretical model (Kuroda et al., 2001). Indeed, the reduction of phosphatase activity was implicated in LTD (Launey et al., 2004). We previously demonstrated that another inhibitory molecule, Raf-kinase inhibitory protein, was involved in regulating the PKC-dependent activation of the MAPK pathway for LTD (Yamamoto et al., 2012). In addition, PTPRR, a MAPK-specific tyrosine phosphatase, was recently shown to act to maintain low basal MAPK activity and to create an optimal

window to boost MAPK activity upon LTD stimulation (Erkens et al., 2015). In the present study, we found that DGK $\zeta$  is involved in LTD by its anchoring function that positively regulates PKC $\alpha$  localization, by its kinase function that negatively regulates PKC $\alpha$  activity, and by its ability to receive inverse regulation from activated PKC $\alpha$  to release PKC $\alpha$ . Similar functional and physical interactions may work to achieve the local and fine activation of signaling molecules required for synaptic plasticity.

### References

- Baumgärtel K, Mansuy IM (2012) Neural functions of calcineurin in synaptic plasticity and memory. *Learn Mem* 19:375–384. [CrossRef Medline](#)
- Belmeguenai A, Hansel C (2005) A role for protein phosphatases 1, 2A, and 2B in cerebellar long-term potentiation. *J Neurosci* 25:10768–10772. [CrossRef Medline](#)
- Brenman JE, Christopherson KS, Craven SE, McGee AW, Bredt DS (1996) Cloning and characterization of postsynaptic density 93, a nitric oxide synthase interacting protein. *J Neurosci* 16:7407–7415. [Medline](#)
- Cai J, Abramovici H, Gee SH, Topham MK (2009) Diacylglycerol kinases as sources of phosphatidic acid. *Biochim Biophys Acta* 1791:942–948. [CrossRef Medline](#)
- Citri A, Malenka RC (2008) Synaptic plasticity: multiple forms, functions, and mechanisms. *Neuropsychopharmacology* 33:18–41. [CrossRef Medline](#)
- Coesmans M, Weber JT, De Zeeuw CI, Hansel C (2004) Bidirectional parallel fiber plasticity in the cerebellum under climbing fiber control. *Neuron* 44:691–700. [CrossRef Medline](#)
- De Zeeuw CI, Hansel C, Bian F, Koekkoek SK, van Alphen AM, Linden DJ, Oberdick J (1998) Expression of a protein kinase C inhibitor in Purkinje cells blocks cerebellar LTD and adaptation of the vestibulo-ocular reflex. *Neuron* 20:495–508. [CrossRef Medline](#)
- Endo S, Launey T (2003) ERKs regulate PKC-dependent synaptic depression and declustering of glutamate receptors in cerebellar Purkinje cells. *Neuropharmacology* 45:863–872. [CrossRef Medline](#)
- Erkens M, Tanaka-Yamamoto K, Cheron G, Márquez-Ruiz J, Prigogine C, Schepens JT, Nadif Kasri N, Augustine GJ, Hendriks WJ (2015) Protein tyrosine phosphatase receptor type R is required for Purkinje cell responsiveness in cerebellar long-term depression. *Mol Brain* 8:1. [CrossRef Medline](#)
- Erlendsson S, Rathje M, Heidarsson PO, Poulsen FM, Madsen KL, Teilum K, Gether U (2014) Protein interacting with C-kinase 1 (PICK1) binding promiscuity relies on unconventional PSD-95/discs-large/ZO-1 homology (PDZ) binding modes for nonclass II PDZ ligands. *J Biol Chem* 289:25327–25340. [CrossRef Medline](#)
- Finch EA, Tanaka K, Augustine GJ (2012) Calcium as a trigger for cerebellar long-term synaptic depression. *Cerebellum* 11:706–717. [CrossRef Medline](#)
- Fukunaga K, Muller D, Ohmitsu M, Bakó E, DePaoli-Roach AA, Miyamoto E (2000) Decreased protein phosphatase 2A activity in hippocampal long-term potentiation. *J Neurochem* 74:807–817. [CrossRef Medline](#)
- Gundlfinger A, Kapfhammer JP, Kruse F, Leitges M, Metzger F (2003) Different regulation of Purkinje cell dendritic development in cerebellar slice cultures by protein kinase  $\alpha$  and  $\beta$ . *J Neurobiol* 57:95–109. [CrossRef Medline](#)
- Hanawa H, Kelly PF, Nathwani AC, Persons DA, Vandergriff JA, Hargrove P, Vanin EF, Nienhuis AW (2002) Comparison of various envelope proteins for their ability to pseudotype lentiviral vectors and transduce primitive hematopoietic cells from human blood. *Mol Ther* 5:242–251. [CrossRef Medline](#)
- Hartell NA (1994) cGMP acts within cerebellar Purkinje cells to produce long term depression via mechanisms involving PKC and PKG. *Neuroreport* 5:833–836. [CrossRef Medline](#)
- Hartmann J, Dragicevic E, Adelsberger H, Henning HA, Sumser M, Abramowitz J, Blum R, Dietrich A, Freichel M, Flockerzi V, Birnbaumer L, Konnerth A (2008) TRPC3 channels are required for synaptic transmission and motor coordination. *Neuron* 59:392–398. [CrossRef Medline](#)
- Hirano T (2013) Long-term depression and other synaptic plasticity in the cerebellum. *Proc Jpn Acad Ser B Phys Biol Sci* 89:183–195. [CrossRef Medline](#)
- Hozumi Y, Ito T, Nakano T, Nakagawa T, Aoyagi M, Kondo H, Goto K

- (2003) Nuclear localization of diacylglycerol kinase  $\zeta$  in neurons. *Eur J Neurosci* 18:1448–1457. [CrossRef Medline](#)
- Huganir RL, Nicoll RA (2013) AMPARs and synaptic plasticity: the last 25 years. *Neuron* 80:704–717. [CrossRef Medline](#)
- Ito M (2002) The molecular organization of cerebellar long-term depression. *Nat Rev Neurosci* 3:896–902. [CrossRef Medline](#)
- Khoutorsky A, Yanagiya A, Gkogkas CG, Fabian MR, Prager-Khoutorsky M, Cao R, Gamache K, Bouthiette F, Parsyan A, Sorge RE, Mogil JS, Nader K, Lacaille JC, Sonenberg N (2013) Control of synaptic plasticity and memory via suppression of poly(A)-binding protein. *Neuron* 78:298–311. [CrossRef Medline](#)
- Kim K, Yang J, Zhong XP, Kim MH, Kim YS, Lee HW, Han S, Choi J, Han K, Seo J, Prescott SM, Topham MK, Bae YC, Koretzky G, Choi SY, Kim E (2009) Synaptic removal of diacylglycerol by DGK $\zeta$  and PSD-95 regulates dendritic spine maintenance. *EMBO J* 28:1170–1179. [CrossRef Medline](#)
- Kim K, Yang J, Kim E (2010) Diacylglycerol kinases in the regulation of dendritic spines. *J Neurochem* 112:577–587. [CrossRef Medline](#)
- Kim MH, Choi J, Yang J, Chung W, Kim JH, Paik SK, Kim K, Han S, Won H, Bae YS, Cho SH, Seo J, Bae YC, Choi SY, Kim E (2009) Enhanced NMDA receptor-mediated synaptic transmission, enhanced long-term potentiation, and impaired learning and memory in mice lacking IRSp53. *J Neurosci* 29:1586–1595. [CrossRef Medline](#)
- Kim T, Tanaka-Yamamoto K (2013) Mechanisms producing time course of cerebellar long-term depression. *Neural Netw* 47:32–35. [CrossRef Medline](#)
- Kim Y, Kim T, Rhee JK, Lee D, Tanaka-Yamamoto K, Yamamoto Y (2015) Selective transgene expression in cerebellar Purkinje cells and granule cells using adeno-associated viruses together with specific promoters. *Brain Res* 1620:1–16. [CrossRef Medline](#)
- Kohda K, Kakegawa W, Matsuda S, Yamamoto T, Hirano H, Yuzaki M (2013) The  $\delta 2$  glutamate receptor gates long-term depression by coordinating interactions between two AMPA receptor phosphorylation sites. *Proc Natl Acad Sci U S A* 110:E948–E957. [CrossRef Medline](#)
- Kondo T, Kakegawa W, Yuzaki M (2005) Induction of long-term depression and phosphorylation of the  $\delta 2$  glutamate receptor by protein kinase C in cerebellar slices. *Eur J Neurosci* 22:1817–1820. [CrossRef Medline](#)
- Kuroda S, Schweighofer N, Kawato M (2001) Exploration of signal transduction pathways in cerebellar long-term depression by kinetic simulation. *J Neurosci* 21:5693–5702. [Medline](#)
- Launey T, Endo S, Sakai R, Harano J, Ito M (2004) Protein phosphatase 2A inhibition induces cerebellar long-term depression and declustering of synaptic AMPA receptor. *Proc Natl Acad Sci U S A* 101:676–681. [CrossRef Medline](#)
- Le TD, Shirai Y, Okamoto T, Tatsukawa T, Nagao S, Shimizu T, Ito M (2010) Lipid signaling in cytosolic phospholipase A2 $\alpha$ -cyclooxygenase-2 cascade mediates cerebellar long-term depression and motor learning. *Proc Natl Acad Sci U S A* 107:3198–3203. [CrossRef Medline](#)
- Leitges M, Kovac J, Plomann M, Linden DJ (2004) A unique PDZ ligand in PKC $\alpha$  confers induction of cerebellar long-term synaptic depression. *Neuron* 44:585–594. [CrossRef Medline](#)
- Leonard TA, Różycki B, Saidi LF, Hummer G, Hurley JH (2011) Crystal structure and allosteric activation of protein kinase C  $\beta$ II. *Cell* 144:55–66. [CrossRef Medline](#)
- Lev-Ram V, Wong ST, Storm DR, Tsien RY (2002) A new form of cerebellar long-term potentiation is postsynaptic and depends on nitric oxide but not cAMP. *Proc Natl Acad Sci U S A* 99:8389–8393. [CrossRef Medline](#)
- Linden DJ, Connor JA (1991) Participation of postsynaptic PKC in cerebellar long-term depression in culture. *Science* 254:1656–1659. [CrossRef Medline](#)
- Luo B, Prescott SM, Topham MK (2003a) Protein kinase C alpha phosphorylates and negatively regulates diacylglycerol kinase zeta. *J Biol Chem* 278:39542–39547. [CrossRef Medline](#)
- Luo B, Prescott SM, Topham MK (2003b) Association of diacylglycerol kinase zeta with protein kinase C alpha: spatial regulation of diacylglycerol signaling. *J Cell Biol* 160:929–937. [CrossRef Medline](#)
- McGee AW, Topinka JR, Hashimoto K, Petralia RS, Kakizawa S, Kauer FW, Aguilera-Moreno A, Wenthold RJ, Kano M, Brecht DS, Kauer F (2001) PSD-93 knock-out mice reveal that neuronal MAGUKs are not required for development or function of parallel fiber synapses in cerebellum. *J Neurosci* 21:3085–3091. [Medline](#)
- Miyata M, Finch EA, Khiroug L, Hashimoto K, Hayasaka S, Oda SI, Inouye M, Takagishi Y, Augustine GJ, Kano M (2000) Local calcium release in dendritic spines required for long-term synaptic depression. *Neuron* 28:233–244. [CrossRef Medline](#)
- Perez JL, Khatri L, Chang C, Srivastava S, Osten P, Ziff EB (2001) PICK1 targets activated protein kinase C $\alpha$  to AMPA receptor clusters in spines of hippocampal neurons and reduces surface levels of the AMPA-type glutamate receptor subunit 2. *J Neurosci* 21:5417–5428. [Medline](#)
- Rincón E, Gharbi SI, Santos-Mendoza T, Mérida I (2012) Diacylglycerol kinase zeta: at the crossroads of lipid signaling and protein complex organization. *Prog Lipid Res* 51:1–10. [CrossRef Medline](#)
- Rizzo MA, Shome K, Vasudevan C, Stolz DB, Sung TC, Frohman MA, Watkins SC, Romero G (1999) Phospholipase D and its product, phosphatidic acid, mediate agonist-dependent raf-1 translocation to the plasma membrane and the activation of the mitogen-activated protein kinase pathway. *J Biol Chem* 274:1131–1139. [CrossRef Medline](#)
- Rizzo MA, Shome K, Watkins SC, Romero G (2000) The recruitment of Raf-1 to membranes is mediated by direct interaction with phosphatidic acid and is independent of association with Ras. *J Biol Chem* 275:23911–23918. [CrossRef Medline](#)
- Sakane F, Imai S, Kai M, Yasuda S, Kanoh H (2007) Diacylglycerol kinases: why so many of them? *Biochim Biophys Acta* 1771:793–806. [CrossRef Medline](#)
- Seo J, Kim K, Jang S, Han S, Choi SY, Kim E (2012) Regulation of hippocampal long-term potentiation and long-term depression by diacylglycerol kinase zeta. *Hippocampus* 22:1018–1026. [CrossRef Medline](#)
- Staudinger J, Lu J, Olson EN (1997) Specific interaction of the PDZ domain protein PICK1 with the COOH terminus of protein kinase C- $\alpha$ . *J Biol Chem* 272:32019–32024. [CrossRef Medline](#)
- Steinberg JP, Takamiya K, Shen Y, Xia J, Rubio ME, Yu S, Jin W, Thomas GM, Linden DJ, Huganir RL (2006) Targeted in vivo mutations of the AMPA receptor subunit GluR2 and its interacting protein PICK1 eliminate cerebellar long-term depression. *Neuron* 49:845–860. [CrossRef Medline](#)
- Takács J, Gombos G, Görcs T, Becker T, de Barry J, Hämori J (1997) Distribution of metabotropic glutamate receptor type 1a in Purkinje cell dendritic spines is independent of the presence of presynaptic parallel fibers. *J Neurosci Res* 50:433–442. [CrossRef Medline](#)
- Tanaka K, Augustine GJ (2008) A positive feedback signal transduction loop determines timing of cerebellar long-term depression. *Neuron* 59:608–620. [CrossRef Medline](#)
- Torashima T, Okoyama S, Nishizaki T, Hirai H (2006) In vivo transduction of murine cerebellar Purkinje cells by HIV-derived lentiviral vectors. *Brain Res* 1082:11–22. [CrossRef Medline](#)
- Wang SS, Khiroug L, Augustine GJ (2000) Quantification of spread of cerebellar long-term depression with chemical two-photon uncaging of glutamate. *Proc Natl Acad Sci U S A* 97:8635–8640. [CrossRef Medline](#)
- Yamamoto Y, Lee D, Kim Y, Lee B, Seo C, Kawasaki H, Kuroda S, Tanaka-Yamamoto K (2012) Raf kinase inhibitory protein is required for cerebellar long-term synaptic depression by mediating PKC-dependent MAPK activation. *J Neurosci* 32:14254–14264. [CrossRef Medline](#)
- Yoshida T, Fukaya M, Uchigashima M, Miura E, Kamiya H, Kano M, Watanabe M (2006) Localization of diacylglycerol lipase- $\alpha$  around postsynaptic spine suggests close proximity between production site of an endocannabinoid, 2-arachidonoyl-glycerol, and presynaptic cannabinoid CB1 receptor. *J Neurosci* 26:4740–4751. [CrossRef Medline](#)
- Zhong XP, Hainey EA, Olenchock BA, Jordan MS, Maltzman JS, Nichols KE, Shen H, Koretzky GA (2003) Enhanced T cell responses due to diacylglycerol kinase  $\zeta$  deficiency. *Nat Immunol* 4:882–890. [CrossRef Medline](#)